Journal of Medicinal Chemistry

Article

Cite This: J. Med. Chem. XXXX, XXX, XXX−XXX

pubs.acs.org/jmc

Synthesis, Biological Evaluation, Structure−Activity Relationship, and Mechanism of Action Studies of Quinoline−Metronidazole Derivatives Against Experimental Visceral Leishmaniasis

Akanksha Upadhyay,[†,∥,⊥] Pragya Chandrakar,[‡,∥,⊥] Sampa Gupta,[†,∥] Naveen Parmar,[‡,∥] Sandeep Kumar Singh,[§,∥] Mamunur Rashid,[§,∥] Pragati Kushwaha,[†,∥] Muhammad Wahajuddin,[§,∥] Koneni V. Sashidhara,[*,†,∥] and Susanta Kar[*,‡,∥]

[†]Medicinal and Process Chemistry Division, [‡]Parasitology Division, and [§]Pharmacokinetics and Metabolism Division, CSIR-Central Drug Research Institute, BS-10/1, Sector 10, Jankipuram Extension, Sitapur Road, Lucknow 226031, India

[∥]Academy of Scientific and Innovative Research (AcSIR), Anusandhan Bhawan, New Delhi 110025, India

Supporting Information

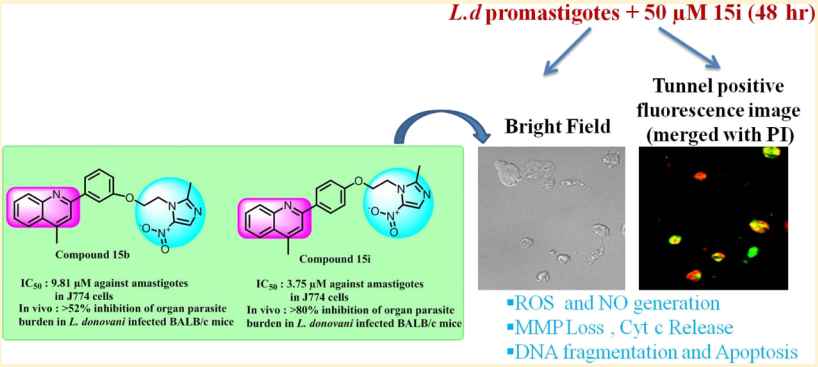

ABSTRACT: In our efforts to identify novel chemical scaffolds for the development of antileishmanial agents, a series of quinoline−metronidazole hybrid compounds was synthesized and tested against the murine model of visceral leishmaniasis. Among all synthesized derivatives, **15b** and **15i** showed significant antileishmanial efficacy against both extracellular promastigote (IC_{50} 9.54 and 5.42 μM, respectively) and intracellular amastigote (IC_{50} 9.81 and 3.75 μM, respectively) forms of *Leishmania donovani* with negligible cytotoxicity toward the host (J774 macrophages, Vero cells). However, compound **15i** effectively inhibited the parasite burden in the liver and spleen (>80%) of infected BALB/c mice. Mechanistic studies revealed that **15i** triggers oxidative stress which induces bioenergetic collapse and apoptosis of the parasite by decreasing ATP production and mitochondrial membrane potential. Structure−activity analyses and pharmacokinetic studies suggest **15i** as a promising antileishmanial lead and emphasize the importance of quinoline−metronidazole series as a suitable platform for the future development of antileishmanial agents.

INTRODUCTION

World Health Organization (WHO) classifies leishmaniasis as one of the most neglected tropical human diseases of global health concern. Visceral leishmaniasis (VL) is a life-threatening disease caused by the obligate intracellular parasites *Leishmania donovani*, *Leishmania infantum* (syn. *Leishmania chagasi*).[1] VLs is nearly always fatal, if not treated; as this disease confers detrimental effects on vital organs like the liver and spleen.[2,3] According to the recent report of WHO, leishmaniasis is prevalent in approximately 90 countries that include areas of India, Nepal, Bangladesh, Sudan, South Sudan, Ethiopia, and Brazil. It is estimated that approximately 70 000 deaths and 1.5−2 million new cases occur every year because of leishmaniasis.[4] Because of the lack of a potent vaccine, chemotherapy emerges as the only approach to cure different types of leishmanial infection. Pentavalent antimonial-based drugs such as sodium stibogluconate, meglumine antimoniate, and other chemotherapeutics like amphotericin B, paromomycin, and pentamidine are the mainstays of antileishmanial chemotherapy.[5−7] However, these drug treatments entail high costs, involve prolonged administration, and even exhibit side-effects like nephrotoxicity, ototoxicity, hepatotoxicity.[6] Additionally, the gradual increase in the resistance of parasite strains against antileishmanial drugs has limited their use for treatment in endemic areas.[8] Miltefosine is the only available oral drug for the first-line therapy of VL[9] as well as cutaneous leishmaniasis,[10] yet its usage involves several drawbacks such as high price, potential fetotoxicity, and teratogenicity.[11] In the search for more effective drugs against VL and other "neglected

Received: April 12, 2019

DOI: 10.1021/acs.jmedchem.9b00628
J. Med. Chem. XXXX, XXX, XXX−XXX

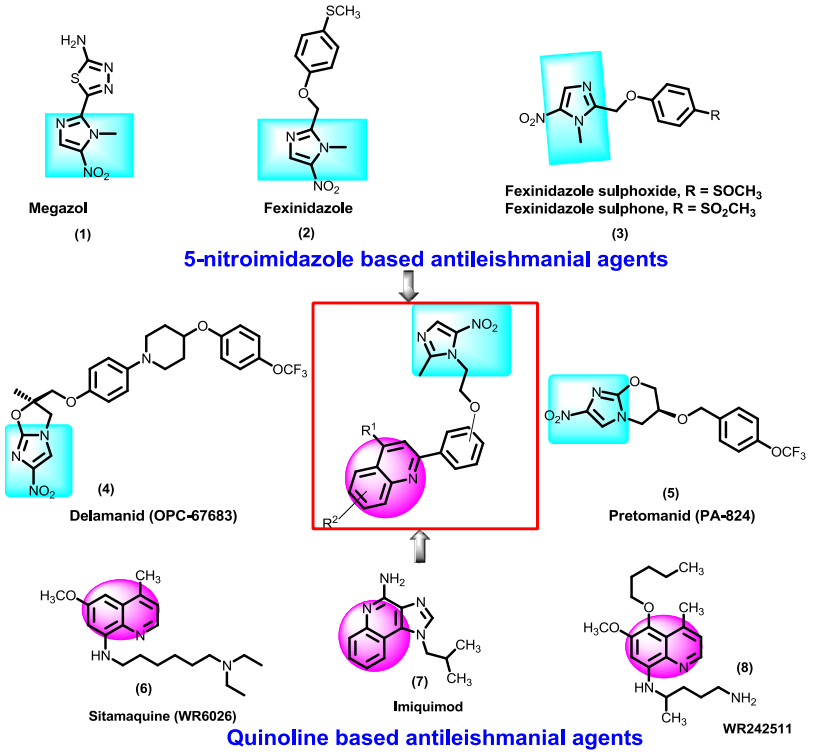

Figure 1. Strategy for designing of quinoline−nitroimidazole hybrids.

tropical diseases", researchers have reassessed the therapeutic value of nitroheterocyclic compounds. In particular, nitro-containing imidazoles like nitroimidazo-oxazine and nitro-imidazooxazole delamanid were shown to have effective antileishmanial efficacy.[12,13] Moreover, the 5-nitroimidazole, fexinidazole is now in clinical trials while back-up nitro-imidazoles, such as DNDI-VL-2098 are at an advanced stage of preclinical development for use in the treatment of VL.[14,15] Research suggests that reduction of the nitro group of nitroimidazoles in pathogens lead to the formation of reactive metabolic intermediates that covalently bind with DNA and trigger cell death. In *Leishmania*, nitroimidazoles are activated by a novel nitroreductase that results in the generation of reactive nitrogen species, including nitric oxides (NO) that are major effectors of these compounds. Because the des-nitro forms of these compounds were found to be inactive against *L. donovani*, this suggests that the nitrogroup plays a key role in the antileishmanial activity of this series.[16] Quinolines are an important structural motif found in numerous natural products that exhibit diverse biological activities.[17−20] Quinoline derivatives have been found to be active against promastigotes of different *Leishmania* species. Compounds with antileishmanial activity such as sitamaquine and tafenoquine, both 8-aminoquinolines, have been extensively studied in recent decades.[21,22] Different analogues of quinoline conjugated to sulfonamide, hydrazide, and hydrazine are known to exert antileishmanial activity by inducing depolarization of the mitochondrial membrane potential (MMP) in promastigotes.[23] In addition to these, quinoline derivatives exerted their effect by inducing reactive oxygen species (ROS) levels in promastigotes.[24] In view of the above considerations, herein, we introduced the nitroimidazole moieties at the second position of quinolines to generate a novel series of hybrids and checked its efficacy against dual life stages of the *L. donovani* parasite. Figure 1 shows the chemical structures of some representative drug leads that contain a quinoline or nitroimidazole in their molecular framework and forms the basis of our designed prototype hybrid. The concept of molecular hybridization was utilized to incorporate them in one molecular platform, in order to produce new hybrid architecture with better efficacy and less toxicity.

RESULTS AND DISCUSSIONS

Chemistry. Our multistep synthetic route is shown in Scheme 1. The synthesis of the proposed prototype was initiated by the tosylation of metronidazole (MET-OH) **9** with excess use of toluene sulphonyl chloride (**10**) in the presence of triethylamine in CH_2Cl_2(10 mL) at 0 °C, afforded the MET-OTs **11** in good yield.[25] Then, the MET-OTs **11** was treated with 3-hydroxyacetophenone **12a** and 4-hydroxyacetophenone **12b** in the presence of K_2CO_3 in DMF at room temperature yielded the desired products **13a** and **13b**, respectively.[26] Further, these compounds were treated with various substituted 2-aminoarylketones in the presence of TFA at 120 °C for 3 h.[27] Under the present reaction conditions, **13a** or **13b** with various substituted 2-aminoarylketones **14** proceeded smoothly and furnished the corresponding products **15a−15m** in good to moderate yield.[28]

In Vitro Antileishmanial Activity of Quinoline−Metronidazole Derivatives. To assess the antileishmanial potency of quinoline−metronidazole derivatives, inhibition of promastigotes and intracellular amastigotes of *L. donovani* was tested initially at two concentrations, that is, 25 and 50 μM (Table 1) for 48 h. To check these, we used luciferase expressing *L. donovani* parasite and cell viability of both promastigotes and intracellular amastigotes was assessed in terms of relative luciferase units. Based on preliminary screening, we found compounds **15b**, **15h**, and **15i** to be maximally active against the promastigote stage of the parasite

DOI: 10.1021/acs.jmedchem.9b00628
J. Med. Chem. XXXX, XXX, XXX−XXX

Scheme 1. Synthesis of Quinoline−Metronidazole Conjugates (15a−15m)[a]

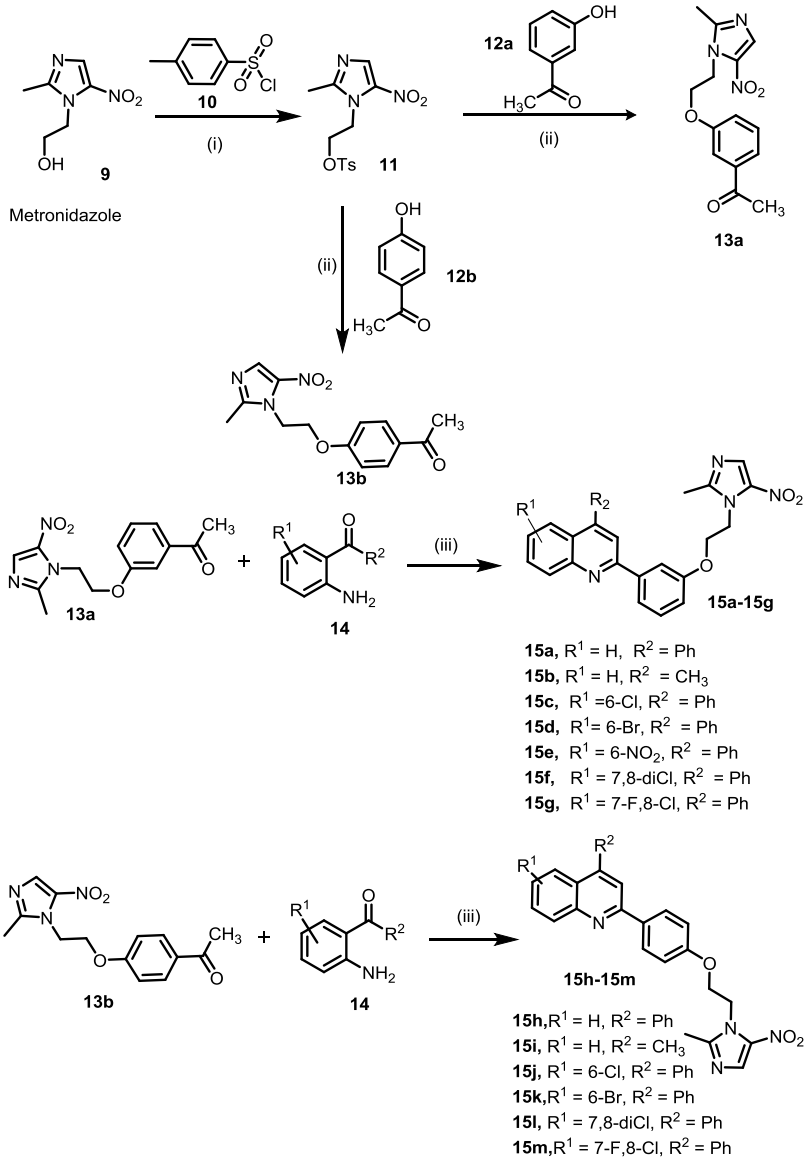

[a]Reagents and conditions: (i) Et_3N, DCM, 0 °C, 5 h. (ii) K_2CO_3, DMF, 35−40 °C, 24 h (iii) TFA, 120 °C, 3 h.

with inhibition rates between 93 and 95% at 50 μM (Table 1). Most of the compounds showed less to moderate activity against the intracellular amastigote form as well, with inhibition ranging from 23 to 67% at 50 μM (Table 1). From the aforementioned compounds, **15b** and **15i** were found to exhibit significant activity against amastigotes, with >93% parasite killing at 50 μM concentration (Table 1). These quinoline−metronidazole hybrids displayed superior antileishmanial activity in comparison to their parent subunits (i.e., quinoline and metronidazole) which showed 83.6 and 68.1% antiamastigote killing, respectively, at 50 μM concentration.

The antileishmanial activity of most active compounds **15b** and **15i** was measured in time as well as dose-dependent fashion against *L. donovani* promastigotes and amastigotes by MTT and luciferase assay, respectively. Dose- and time-dependent inhibition against promastigotes were observed by both compounds **15b** and **15i**, where maximum inhibition was >93% as determined by luciferase and MTT assay (Figure 2A,B). In addition to these, half-maximal inhibition (IC_{50}) concentrations of **15b** and **15i** against promastigotes were 9.54 ± 0.73 and 5.42 ± 0.45 μM as determined by luciferase assay. This was comparable with the antipromastigote IC_{50} of both these compounds (9.4 ± 1.2 and 5.3 ± 0.65 μM for **15b** and **15i**, respectively) as determined by MTT assay. Similarly, different concentrations of **15b** and **15i** were found to successfully inhibit the intracellular multiplication of the parasite in a dose-dependent fashion in J774 macrophages, where maximum elimination of amastigotes was observed at a dose of 50 μM by both luciferase assays (>96%, Figure 2C) and Giemsa staining of intracellular amastigotes (>93%, Figure 2D). Half-maximal inhibition concentrations (IC_{50}) of **15b** and **15i** against intracellular amastigotes, were found to be 9.81 ± 2.05 and 3.75 ± 0.68 μM by luciferase assay and 9.09 ± 1.04 and 4.06 ± 0.70 μM by Giemsa staining, respectively, at 48 h, both of which are lesser than that of their parent subunits metronidazole, or quinoline (IC_{50}: 28.4 and 11.6 μM, respectively). Moreover, they are either equivalent to, or lesser than the IC_{50} of miltefosine (standard chemotherapeutic

DOI: 10.1021/acs.jmedchem.9b00628
J. Med. Chem. XXXX, XXX, XXX−XXX

Table 1. In Vitro Antileishmanial Efficacy of Compounds[a]

		promastigotes		intracellular amastigotes	
s. no.	compound code	concentration (μM)	% inhibition	concentration (μM)	% inhibition
1	**15a**	50	63 ± 7.2	50	66.4 ± 7.5
		25	43 ± 5.9	25	31.2 ± 5
2	**15b**	50	94.7 ± 2.1	50	93.2 ± 3.8
		25	77.8 ± 8.2	25	75.2 ± 7.9
3	**15c**	50	58.2 ± 7.1	50	59.2 ± 9.9
		25	41.2 ± 6	25	38.2 ± 6.1
4	**15d**	50	60.8 ± 8.8	50	65.3 ± 7.2
		25	30.2 ± 4.1	25	29.5 ± 6.3
5	**15e**	50	NSI	50	10.4 ± 2
		25	NSI	25	NSI
6	**15f**	50	26 ± 3.9	50	NSI
		25	12.3 ± 4.6	25	NSI
7	**15g**	50	NSI	50	12.1 ± 3.3
		25	NSI	25	NSI
8	**15h**	50	93.2 ± 4.4	50	67.7 ± 8.2
		25	78.2 ± 9.1	25	45.3 ± 5.2
9	**15i**	50	94.4 ± 1.2	50	93.8 ± 2.5
		25	85.8 ± 6.4	25	83.2 ± 7.3
10	**15j**	50	65.8 ± 7.2	50	64.4 ± 7
		25	45.3 ± 5	25	34.2 ± 5.2
11	**15k**	50	63.9 ± 7.3	50	60.3 ± 7.2
		25	41.3 ± 5.2	25	33.8 ± 4.8
12	**15l**	50	61.7 ± 7.7	50	27.2 ± 4.5
		25	38.2 ± 5.1	25	12.1 ± 3
13	**15m**	50	59.1 ± 6.4	50	63.6 ± 7.2
		25	34.4 ± 5.1	25	23.4 ± 4.3
14	**metronidazole**	50	62.2 ± 5.2	50	68.1 ± 5.8
		25	41.3 ± 3.8	25	31.2 ± 3.5
15	**quinoline**	50	80.2 ± 5.2	50	83.6 ± 4.3
		25	42.4 ± 3.1	25	64.5 ± 3.8
16	**miltefosine**	50	99.5 ± 0.2	50	99.2 ± 0.3
		25	97.2 ± 0.7	25	98.3 ± 0.7

[a]Percentages of inhibition are expressed as mean ± standard deviation for each compound of three individual experiments (at least) performed in duplicates, NSI (no significant inhibition).

regimen for VLs, anti-amastigote IC_{50}: 9.59 μM) (Figure 2C,D). Both these compounds were found to be noncytotoxic and exhibited a higher safety index (SI = CC_{50}/IC_{50}, of **15b** and **15i**, was observed as 12.6 and 17.6 in J774 cells, and 36.05 and 57.9 in Vero cells, respectively, as compared to miltefosine, SI = 5.8 and 5.3 in J774 macrophages and Vero cells, respectively). Both **15b** and **15i** showed much less toxicity toward J774 and Vero cells as >92% cells and >86% cells were viable up to 50 and 100 μM concentrations, respectively. Increasing the concentration of both **15b** and **15i** to 100 μM did not alter their activity against promastigotes and amastigotes significantly and was almost equivalent to the percentage inhibition observed at 50 μM. Thereby, the 50 μM concentration was taken as the MIC (maximum inhibitory concentration) for both **15b** and **15i**. The preliminary in vitro screening revealed that out of the synthesized derivatives, ten compounds exhibited better (58−95%) inhibition at 50 μM concentrations against promastigotes. Interestingly, the hybrids were more active against *L. donovani* as compared to the parental subunits alone, that is, quinoline and metronidazole. The unsubstituted quinoline analog **15h** displayed significant activity (93.2% inhibition) against promastigotes as shown in Table 1. The presence of methyl substitution at R_2 of the quinoline ring enhances activity against promastigotes with lesser cytotoxicity when evaluated and compared to miltefosine as shown in Figure 2A (**15b** and **15i** having IC_{50} = 9.54 ± 0.73 μM and IC_{50} = 5.42 ± 0.45 μM, respectively). Further, these derivatives were tested for their activity against the intracellular amastigotes form. In this screening, again the compounds **15b** and **15i** possessing a methyl group at R_2 position exhibited robust activity against amastigotes with IC_{50} = 9.81 ± 2.05 μM and IC_{50} = 3.75 ± 0.68 μM, respectively, as compared to the standard drug miltefosine. However, the substitution at R_1 position of quinoline had no influence on biological activity. Thus, in terms of preliminary structure−activity relationship (SAR), the methyl substitution at the fourth position, that is, R_2 of the quinoline ring enhanced activity against both the promastigote and amastigote stages of the parasite. Also, both para and meta substitution of the phenyl ring attached to the quinoline ring with the nitroimidazole moiety were pivotal for optimum activity, which could be seen in the case of compounds **15b** and **15i**. A preliminary summary of SAR is schematically represented in Figure 3. These results further led to the evaluation of in vitro pharmacokinetics stability of **15b** and **15i** before proceeding for the determination of antileishmanial efficacy against *L. donovani*-infected BALB/c mice.

DOI: 10.1021/acs.jmedchem.9b00628
J. Med. Chem. XXXX, XXX, XXX−XXX

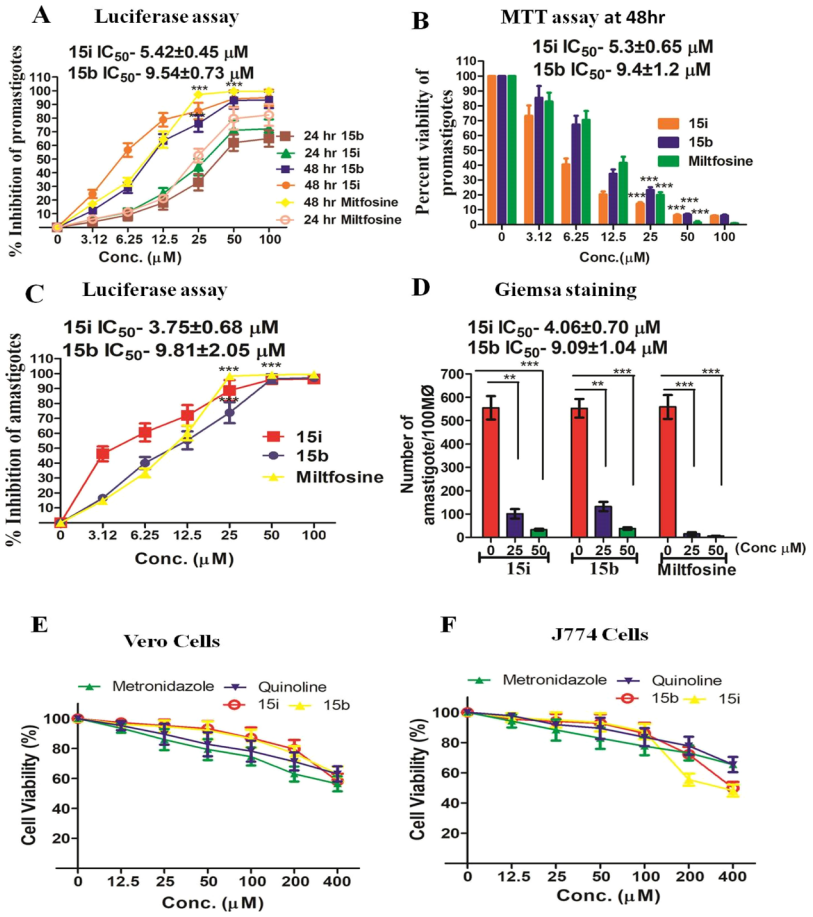

Figure 2. Antileishmanial activity of **15b** and **15i** in in vitro. (A) Percentage inhibition of parasites was assessed by luciferase assay after treatment with **15b** and **15i** at different concentrations for 24 and 48 h. (B) Percent viability/survival of promastigotes was evaluated by MTT assay after treatment with varying concentrations of **15b** and **15i** for 48 h. (C,D) Macrophages were infected with a 1:8 (cell: promastigote) ratio, followed by treatment with different doses of compounds **15b** and **15i** for 48 h, as described in the Experimental Section. The percentage of amastigote inhibition was determined by luciferase assay (C) and the number of intra-macrophagic amastigotes was evaluated by Giemsa staining (D) as described in the Experimental Section. (E,F) Vero cells and J774 macrophages were incubated at varying concentrations of **15b** and **15i** for 48 h and cell viability was checked by the MTT method. Data are represented as means ±SD of individual experiments (n = 3), which were done in replicate. Significance levels are represented as untreated vs **15b**, **15i**-treated groups with 25 and 50 μM doses, $^{**}p < 0.005$, $^{***}p < 0.0001$.

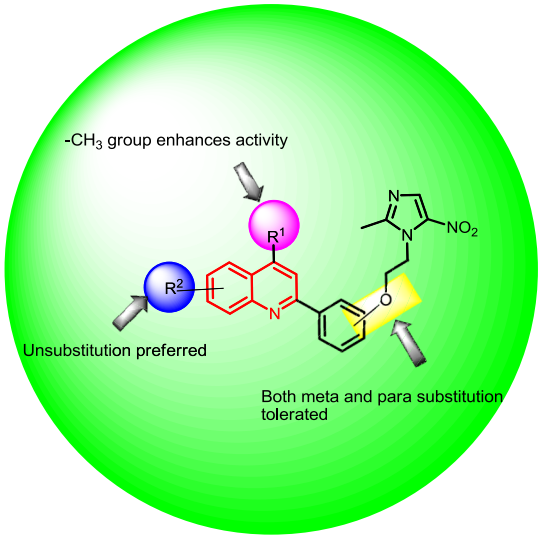

Figure 3. Pictorial representation of SAR of quinoline−metronidazole hybrid.

In Vitro Pharmacokinetic Study. *In Vitro-Simulated Gastric Fluid and Simulated Intestinal Fluid Stability.* The stability of **15b** and **15i** was assessed in simulated gastric fluid (SGF, pH 1.2) and simulated intestinal fluid (SIF, pH 6.5). Both these compounds were found to be stable in gastric fluid as 84.72 ± 2.62% of **15b** and 83.58 ± 0.77% of **15i** remained intact after 2 h of incubation with SGF (Figure 4A).

However, the percentage remaining in the intestinal fluid was found to be only 11.40 ± 0.35 and 43.56 ± 3.84% for **15b** and **15i**, respectively, as observed up to 2 h (Figure 4B). These results demonstrated that compound **15i** was relatively more stable as compared to **15b** in the intestinal fluid.

In Vitro Plasma Stability. Evaluation of plasma stability of **15b** and **15i** in rat plasma is depicted in Figure 4C. The results demonstrate that the compounds were found to be stable as 68.16 ± 0.085% of **15b** and 88.50 ± 3.95% of **15i**, remained intact in rat plasma after 2 h incubation. The results also clearly indicated that compound **15i** was more stable in rat plasma as compared to **15b**.

In Vitro Microsomal Stability. In vitro microsomal stability indicates hepatic clearance (Cl) of drug from the liver. The result of microsomal stability of compound **15b** and **15i** using rat liver microsomes (RLM) is shown in (Figure 4D). The

DOI: 10.1021/acs.jmedchem.9b00628
J. Med. Chem. XXXX, XXX, XXX−XXX

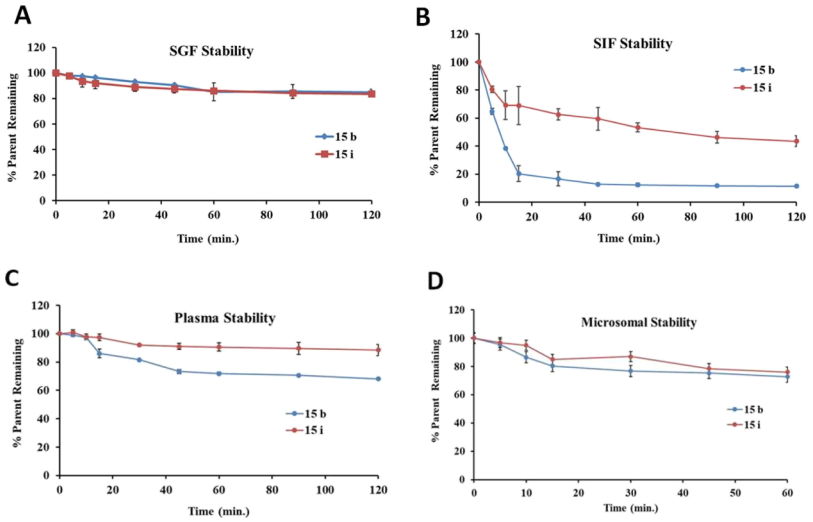

Figure 4. In vitro stability of compounds **15b** and **15i** in simulated gastric (A) and intestinal (B) fluids up to 2 h. In vitro stability of compounds **15b** and **15i** in rat plasma (C) and in RLMs (D).

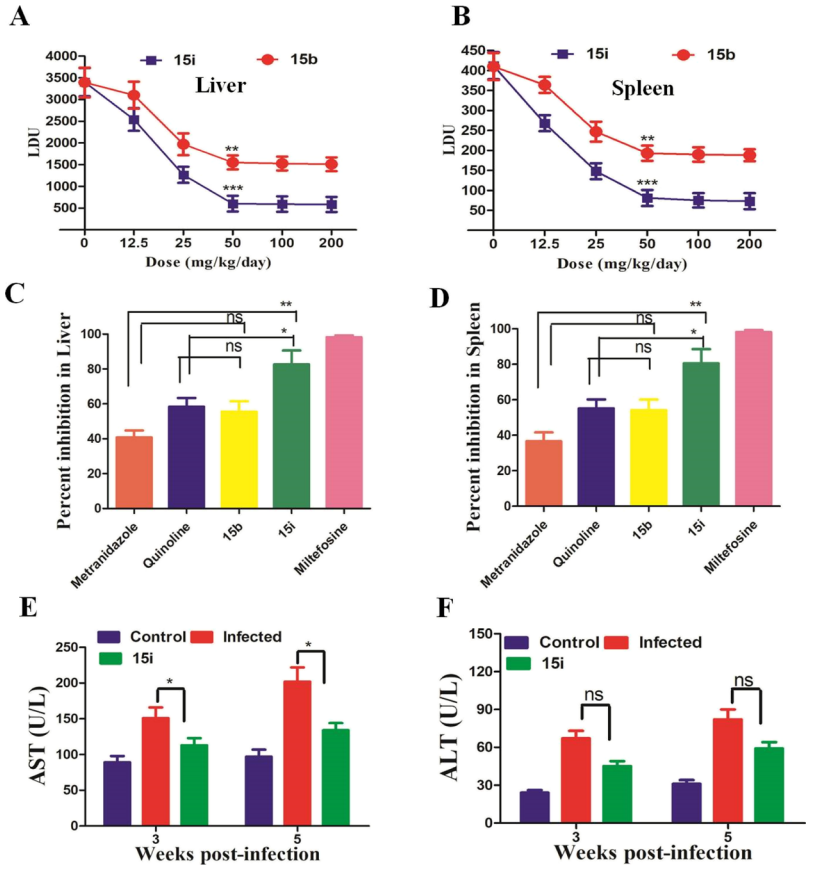

Figure 5. Effect of **15b** and **15i** treatment in controlling in vivo infection: 15 day-infected BALB/c mice were treated with different doses of **15b** and **15i** as indicated. Mice of different experimental groups (n = 5 mice per group), were killed for the determination of hepatic (A) and splenic (B) parasite burden by the stamp-smear method and represented as Leishman Donovan units (LDU). The in vivo safety index of **15b** and **15i** was determined by assessment of serological markers. (C,D) 15 day-infected BALB/c mice were treated with 50 mg/kg of quinoline, metronidazole, **15b**, **15i** and 25 mg/kg of miltefosine for 5 consecutive days. Mice of different experimental groups (n = 5 mice per group), were sacrificed at day 7 post-treatment for the determination of hepatic (C) and splenic (D) parasite burden by the stamp-smear method and represented as LDU. (E) AST and (F) ALT at various time points in infected and treated BALB/c mice. Data represent mean ± SD (n = 5 mice per group), representative of three independent experiments were performed in replicate. Significance is indicated for untreated vs **15b**, **15i**-treated groups with 50 mg/kg dose; *p < 0.05, **p < 0.005, ***p < 0.0006, ns = nonsignificant.

compounds **15b** and **15i** were found to be intact as 72.77 ± 2.32 and 75.97 ± 0.63%, respectively, after 60 min incubation in RLM. The in vitro half-life ($t_{1/2}$) and related parameters of compound **15b** and **15i** were calculated by plotting the natural

DOI: 10.1021/acs.jmedchem.9b00628
J. Med. Chem. XXXX, XXX, XXX−XXX

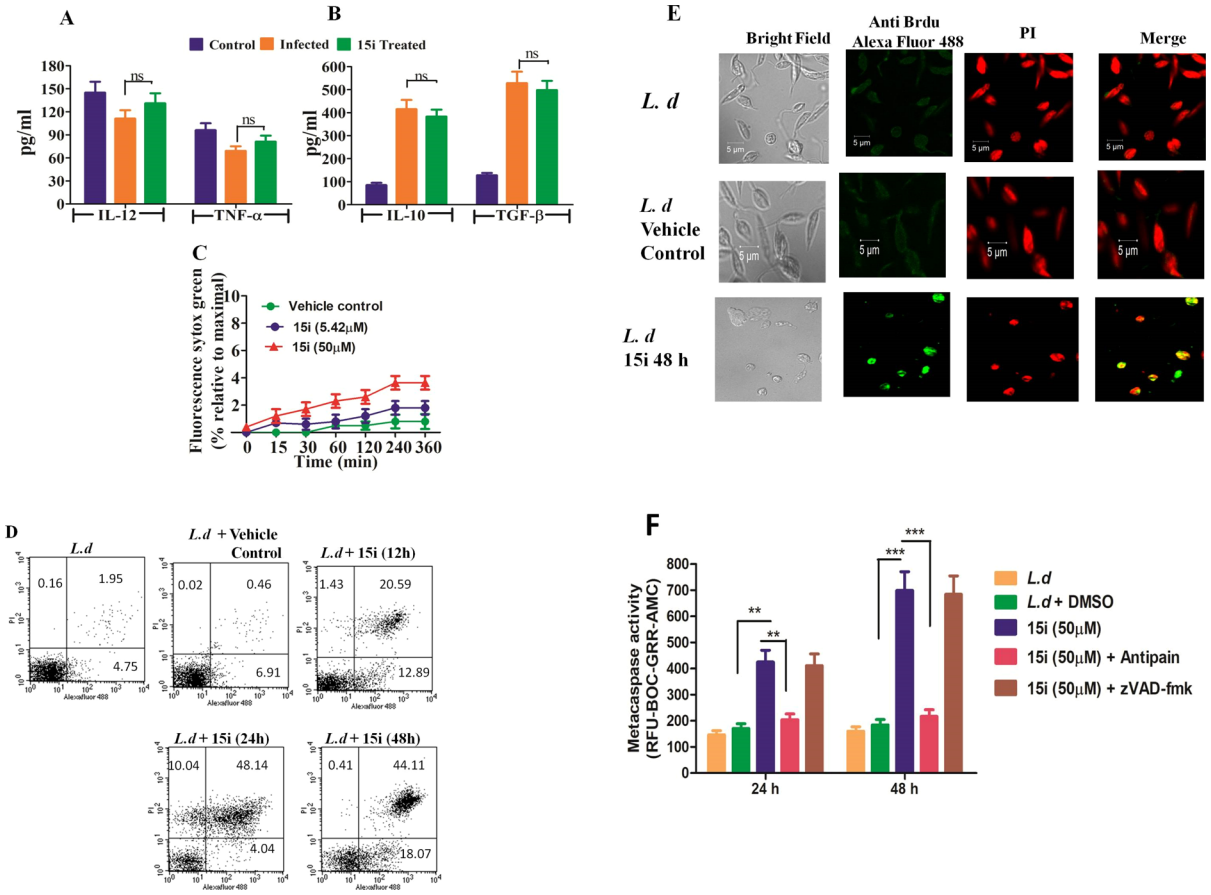

Figure 6. **15i**-treated *L. donovani* promastigotes underwent apoptosis: J774 macrophages infected with *L. donovani* promastigotes (24 h) were further incubated with 50 μM of **15i** for 48 h. (A) Th1 and (B) Th2 cytokines levels in cultured supernatant were evaluated by ELISA. (C) *L. donovani* parasites were incubated with 50 μM of **15i** for different time points and analyzed for membrane permeabilization using the SYTOX dye. Results were represented in percentages to the maximum normalized fluorescence as obtained with 0.1% Triton X-100 used for maximal promastigote permeabilization. (D) Exponential phase *L. donovani* parasite (1×10^6) was incubated at maximum parasite inhibitory concentration of **15i** (50 μM) for 12, 24, and 48 h. Parasites incubated with 0.1% DMSO for 48 h were taken as the vehicle control. After incubation, promastigotes were stained with Annexin-V Alexa Fluor 488 and PI and analyzed by flow cytometry. (E) DNA fragmentation of parasites was analyzed by TUNEL assay. Log phase promastigotes were incubated with either vehicle (48 h) or **15i** (50 μM) for 48 h. TUNEL assay was carried out as mentioned in the Experimental Section. Tunnel-stained parasites were then visualized by both phase contrast, as well as fluorescent microscopy. (F) Fluorogenic substrate BOC-GRR-AMC (*t*-butyloxycarbonyl-Gly-Arg-Arg-AMC) was used to determine metacaspase activity. Log phase promastigotes were treated with DMSO (0.1%), 15i (50 μM) either alone or in parasites pretreated with antipain (1 μM) or zVAD-fmk (100 μM) for 1 h. Activity is expressed as relative fluorescence unit and normalized to mg of protein obtained leishmanial cell lysates. The significance level is determined for the untreated vs treated groups, ns = nonsignificant.

logarithm of the percentage compound remaining versus incubation time up to 60 min. The half-life values of **15b** and **15i** were found to be 2.18 ± 0.32 and 2.50 ± 0.27 h, respectively. Nevertheless, the intrinsic Cl values of compounds **15b** and **15i** were found to be 10.7 ± 1.56 and 9.3 ± 0.99 μL/min/mg, respectively. The abovementioned preclinical stability studies demonstrated that compound **15i** has higher stability under a different set of experimental conditions as compared to compound **15b**.

*In Vivo Activity of Compound **15b** and **15i** Against L. donovani-Infected Mice.* *L. donovani*-infected BALB/c mice (15 days) were administered with compounds **15b** and **15i** via intraperitoneal route (as described in Experimental Section), for five consecutive days with 12.5−200 mg/kg/day dose range and then sacrificed at 7th day after completion of treatment. The parasitic load was determined in the stamp smears obtained from spleen and liver. Both compounds **15b** and **15i** were observed to inhibit parasitic load in the organs of infected BALB/c mice in a dose-dependent fashion (Figure 5A,B). However, dose-dependent antileishmanial activity was different for both the compounds where **15i** exhibited better efficacy as compared to **15b**. Parasitic inhibition by compound **15i** in liver and spleen was observed to be >62% at 25 mg/kg (lower dose), whereas compound **15b** was able to eliminate >50% parasite from liver and spleen at 50 mg/kg dose. For **15i**, maximum inhibition of organ parasite burden was obtained at 50 mg/kg/day dose for 5 consecutive days, where we observed >80.3 and >82.3% inhibition in both splenic and liver parasitic load, respectively, at the 7th day of post-treatment. The inhibition observed was much higher when compared to their parent components (quinoline and metronidazole alone) administered for 5 consecutive days at the dose of 50 mg/kg (Figure 5C,D). We observed 36.6 and 40.8% inhibition of the parasitic load in spleen and liver, respectively, for metronidazole, and 55.2 and 58.2% inhibition of parasite burden in spleen and liver, respectively, for quinoline. Moreover, no significant increase in therapeutic efficacy of **15i** was observed upon increasing the dose to 100 mg/kg (inhibition in spleen

DOI: 10.1021/acs.jmedchem.9b00628
J. Med. Chem. XXXX, XXX, XXX−XXX

and liver parasite burden was 81.7 and 82.5%, respectively) and 200 mg/kg (inhibition in spleen and liver parasite burden was 82.2 and 82.7%, respectively). However, maximum inhibition in liver and splenic parasitic load was found to be 54.14 and 55.5%, respectively, for **15b**, even at a higher dose of (200 mg/kg). Miltefosine used as standard reference drug showed >98% inhibition of parasite burden at a curative dose (25 mg/kg/day for 5 days) in both the spleen and liver of infected BALB/c mice. During the experimental time duration, all mice were found to be alive, healthy, and no marked reduction in weight was observed in any of the experimental groups. Additionally, in order to assess the in vivo safety index, the major serological markers of toxicity, alanine aminotransferase (ALT), and aspartate aminotransferase (AST) levels were also checked in BALB/c mice of different experimental groups. On comparing ALT and AST levels in uninfected and *L. donovani*-infected BALB/c mice at 3rd and 5th week postinfection, we found a significant rise in the serum level of both serological markers ALT and AST in *L. donovani*-infected BALB/c mice, which were measured as 82 and 202 U/L, respectively, after 5th week of infection. On the other hand, levels in control BALB/c mice was measured as 31 and 97 U/L, respectively, at 5th week (Figure 5E,F). Interestingly, treatment with **15i** in infected BALB/c mice clearly reduced the levels of both serological markers at every time period. Nevertheless, levels of both markers remained within the normal range (AST—54 to 298 U/L and ALT—17 to 77 U/L in control animal). These results suggested that **15i** did not induce any hepatotoxicity.

Effect of 15i on Host Immunomodulation As Well As Plasma Membrane Integrity/Programmed Cell Death of *L. donovani* Promastigotes. During infection, *L. donovani* creates a favorable environment by shifting the T-cell responses from healing Th1 to nonhealing Th2 mode that favors the persistence of the parasite inside the host. Thus, redirecting the immune response from Th2 to Th1 mode and boosting immune cells by stimulating Th1-mediated proinflammatory cytokine secretion is a rational approach in leishmanial chemotherapy. To examine whether **15i** was capable of stimulating host immunity, we chose 50 μM dose for in vitro studies, as it induced maximum killing of both promastigote and intracellular amastigote. To evaluate the changes in Th1/Th2 cytokines, J774 macrophages were infected with promastigotes, followed by treatment with **15i** for 48 h and the resulting supernatant was assessed for cytokine estimation. Enzyme-linked immunosorbent assay (ELISA) analysis showed no significant increase in Th1 cytokines (TNF-α and IL-12) or reduction in Th2 cytokines (TGF-β and IL-10) in **15i**-treated macrophages as compared to infected cells (Figure 6A,B). Because **15i** did not induce any apparent host-protective cytokine response, we hypothesized that it could exert its effect by direct killing of *L. donovani* via apoptosis or necrosis.

To address this issue, we first tried to understand whether the compound was inducing plasma membrane permeabilization of *L. donovani* promastigotes by lesion or pore formation that eventually resulted in parasitic cell death from osmolysis or necrosis. We checked for the cytosolic entry of SYTOX green in **15i**-treated parasites, which requires large-sized lesions in the membrane, typical of nonspecific pore formation. *L. donovani* promastigotes were incubated with both IC_{50} as well as MIC of **15i** for different time points and then incubated with the SYTOX green dye. Flow-cytometric analysis revealed that only 3.63% increase in the fluorescence after 4 h treatment with MIC of **15i** as compared to maximum permeabilization achieved with 0.1% Triton X 100, used as the positive control (Figure 6C). Negligible uptake of SYTOX green excluded the possibility of nonspecific pore formation and clearly indicated that **15i** did not kill the parasite via osmolysis-mediated necrosis. The apparent absence of necrotic cell death by **15i** encouraged us to check whether it could trigger apoptotic cell death machinery in the leishmanial parasite, as we previously observed antipromastigote activity of this compound by MTT assay. Phosphatidylserine externalization is a hallmark feature of cells undergoing apoptosis. Therefore, we next detected phosphatidylserine externalization by staining **15i**-treated promastigotes with both Annexin-V-coupled FITC, as well as propidium iodide (PI) to check for apoptosis or necrosis. The dot plots are represented in (Figure 6D), which clearly demonstrated that treatment with **15i** for 24 h could initiate early apoptosis as 52.18% of parasites was found in both Annexin-V/PI positive quadrants. This further increased to 62.18% at 48 h treatment with **15i**. On the other hand, only 7.3% of the promastigotes underwent apoptosis when treated with a vehicle [0.1% dimethyl sulfoxide (DMSO)] which was almost parallel to the control parasite (where 6.7% underwent apoptosis, Figure 6D). Programmed cell death of **15i**-treated parasites was subsequently evaluated at the nuclear level by detecting DNA fragmentation through terminal deoxynucleotidyl transferase dUTP nick end labeling (TUNEL) staining. Promastigotes showed bright green fluorescence denoting TUNEL positivity after treatment with **15i** for 48 h (Figure 6E). In contrast, control and vehicle-treated parasites showed red fluorescence because of counterstaining with PI (Figure 6E). Merged image of the **15i**-treated parasite also appeared as bright yellowish green because of TdT-labeled nuclei, which is indicative of programmed cell death. In addition to DNA degradation, changes in the structure and morphology of the parasites were observed by confocal microscopy. Promastigotes treated with **15i** appeared to be round in shape as compared to untreated promastigotes that were flagellated and elongated, as observed by bright field microscopy. Caspases are the primary executioners of apoptosis in mammalian cells, however, in protozoans, this function is accomplished by its protozoan counterpart, that is, metacaspases. Emerging evidence suggests that metacaspase initiates programmed cell death in leishmanial parasite and its activity is unaffected by caspase inhibitors; however, it is highly sensitive to serine protease inhibitors like antipain or TLCK.[29−32] We, therefore, evaluated the activation of metacaspases by treating *L. donovani* parasites with **15i** for 24 and 48 h, either in the presence or absence of caspase and metacaspase inhibitors. Our results suggested that **15i**-upregulated metacaspase activity by 3.8-fold (at 48 h), as compared to vehicle (0.1% DMSO)-treated parasites. This **15i**-mediated increase in metacaspase activity remained unaffected by the prior treatment of caspase inhibitors (zVAD-fmk, 100 μM) but significantly decreased in the presence of the metacaspase inhibitor (Antipain, 1 μM) (Figure 6F).

15i-Induced Mitochondrial-Programmed Cell Death of the Parasites. Mitochondrial dysfunction and loss in MMP ($\Delta\Psi_m$) are early events in the induction of apoptosis in *L. donovani* parasites that are commonly induced by chemotherapeutic agents.[33] To examine whether **15i** treatment in *L. donovani* promastigotes could change its MMP in a time-dependent fashion, $\Delta\Psi_m$ was evaluated using the fluorescent dye, JC-1. At higher potential, the JC-1 dye forms aggregates and fluoresces red in the mitochondria of control promasti-

DOI: 10.1021/acs.jmedchem.9b00628
J. Med. Chem. XXXX, XXX, XXX−XXX

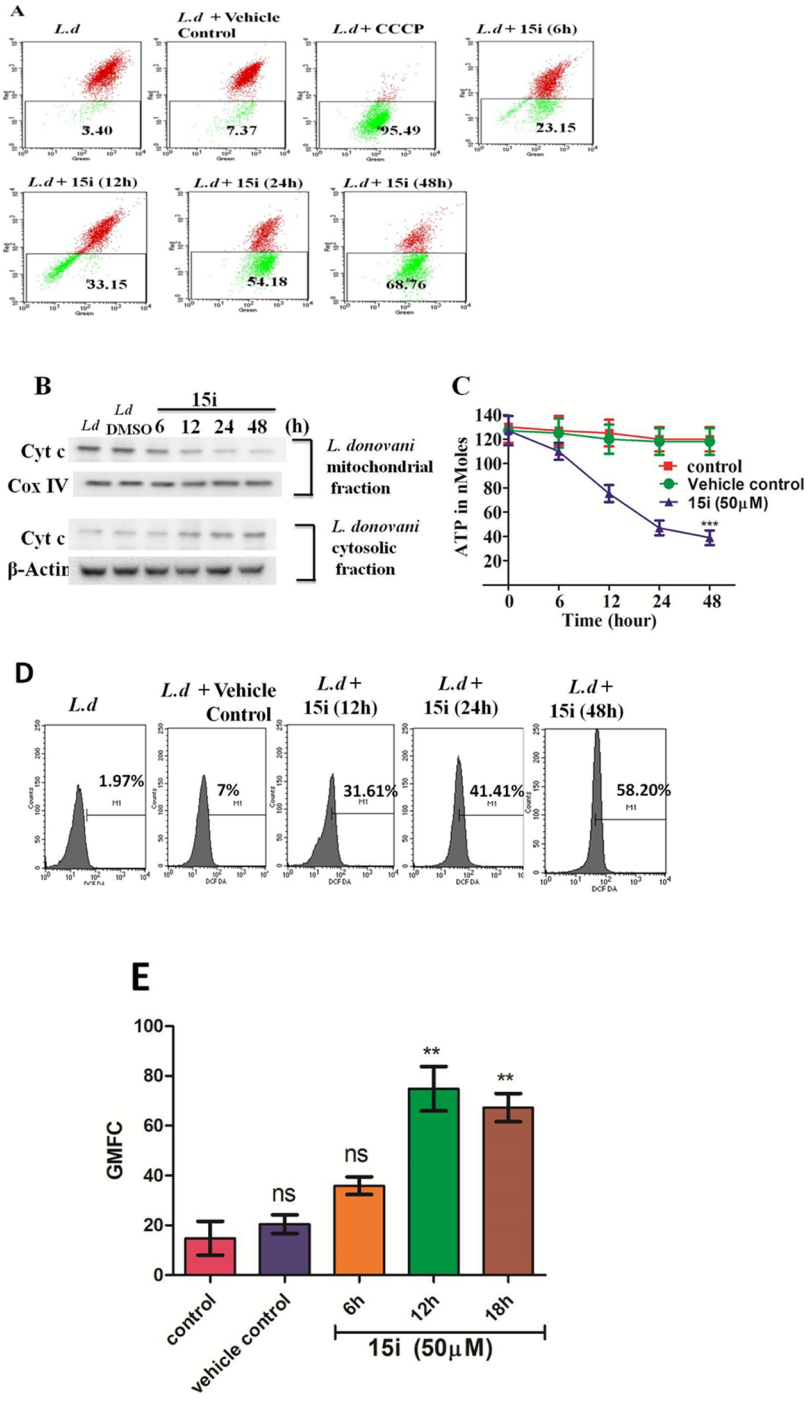

Figure 7. Determination of MMP loss, Cyt *c* release, ATP, ROS, and NO generation in 15i-treated promastigotes. (A) Exponential phase promastigotes were incubated with **15i** (50 μM) for 6−48 h or vehicle (0.1% DMSO). Parasites were also incubated with CCCP (50 μM), as the positive control. Changes in MMP were observed after the addition of the JC-1 dye in flow cytometry. (B) Immunoblot study to check the level of cytochrome *c* in mitochondrial (upper panel) and cytoplasmic (lower panel) fractions isolated from vehicle (0.1% DMSO, 48 h) or 15i-treated parasites (50 μM, 6−48 h). COX-IV and β-tubulin were used as the endogenous controls for mitochondrial and cytosolic fractions, respectively. (C) *L. donovani* parasites were incubated with either 0.1% DMSO or 50 μM of **15i** for 6−48 h. ATP content in the cytosol was determined as mentioned in the Experimental Section. (D) Parasites were untreated, vehicle-treated or treated with **15i** compound at (50 μM) for different time periods and probed with H_2DCFDA (20 μM). ROS generation was measured by flow cytometry as described in the Experimental Section. (E) Log phase *L. donovani* promastigotes were incubated with **15i** (50 μM) for the respective time period followed by labeling with DAF-2DA (40 μM); fluorescence was measured as described in the Experimental Section. Data are expressed as mean of at least 3 independent experiments done in duplicate. The significance level is determined for the untreated vs treated groups, $^{**}p < 0.005$, $^{***}p < 0.0004$, ns = nonsignificant.

gotes. MMP loss is characterized by a shift of fluorescence signal from red to green (595−530 nm) as JC-1 at a lower potential forms monomers and emits green fluorescence in the cytoplasm. The maximum percentage of the control and vehicle-treated promastigotes emitted red fluorescence, indicating functionally intact mitochondria. On the other hand, in **15i**-treated parasites, the fluorescence signal shifted from red to green in a time-dependent fashion, thereby denoting the

DOI: 10.1021/acs.jmedchem.9b00628
J. Med. Chem. XXXX, XXX, XXX−XXX

absence of mitochondrial JC-1 accumulation. Flow cytometric studies showed an increase of 33.15, 54.18, and 68.76% green fluorescent cells at 12−48 h post treatment (Figure 7A). CCCP (mitochondrion uncoupler) was used as a positive control and we observed the fluorescence signal shifted from red to green remarkably in CCCP-treated parasites, which suggested JC-1 sensitivity toward membrane potential in leishmanial cells. This observation strongly suggested that **15i**-mediated disruption of MMP was perpetrated by an intrinsic pathway of apoptosis in *Leishmania* promastigotes. The dissipated mitochondrial membrane results in the release of cytochrome *c* from mitochondria to cytosol, which in turn hampers the effective functioning of the electron transport chain. Immunoblot results suggested that in vehicle-treated promastigotes, mitochondria remains functionally intact and cytochrome *c* is localized in the mitochondrial fraction (Figure 7B). On the contrary, **15i** treatment rapidly induced the cytosolic translocation of cytochrome *c* in the parasite which was evident from an increased cytosolic abundance of cytochrome *c* with gradual disappearance in the mitochondrial fraction (Figure 7B). The loss in membrane potential and leakage of cytochrome *c* directly affects mitochondrial electron transport chain function and ultimately disrupts ATP generation. Consequently, cells may undergo either necrosis or apoptosis. To study the fate of ATP generation in **15i**-treated *L. donovani* promastigotes, we performed bioluminescence assay and found that ATP levels were higher and comparable in control and DMSO-treated promastigotes (120 ± 11 and 118 ± 12 nM, respectively) but was subsequently lower in **15i**-treated parasites (Figure 7C). Maximum inhibition was observed after 48 h treatment with >67% reduction in the ATP level in **15i**-treated parasites as compared to vehicle-treated parasites.

In mammalian cells, increased cellular ROS generation has been known to be responsible for the depolarization of the mitochondrial membrane and subsequent cell death.[34,35] To investigate whether the mitochondrial dysfunction observed in *L. donovani* promastigote treated with **15i** is promoted by ROS generation, we performed flow cytometry using cell-permeable dye 2′,7′-dichlorodihydrofluorescein diacetate (H_2DCFDA), which is widely known as a ROS indicator. While the reduced form of H_2DCFDA does not emit fluorescence, its oxidized fluorescent form 2′,7′-dichlorofluorescein (DCF) can be detected by flow cytometry. Our results showed that after 12 h incubation with **15i** at 50 μM concentrations, ROS generation was increased by 31.6% in the promastigotes which further increased to 41.4 and 58.2% at 24 and 48 h post treatment, respectively. On the contrary, promastigotes treated with the vehicle (0.1% DMSO) showed only 7% ROS positivity (Figure 7D). Similar to ROS, NO is well-known for its antimicrobial effect against a variety of protozoan, bacterial, and viral pathogens.[36−39] For identifying newer and more effective drugs against VL, trypanosomiasis, and tuberculosis, researchers have already reconsidered exploring the therapeutic potential of nitroheterocyclic compounds.[12,13,40] Hence, we proceeded to investigate whether **15i** could induce NO generation for its leishmanicidal action. NO generation was detected by the DAF-2DA dye that, upon binding an oxidized species of NO, results in an irreversible DAF fluorescence, thereby implying local NO formation in living cells at an intracellular level. For these, we treated *L. donovani* promastigotes with **15i** for 6−18 h followed by incubation with 40 μM DAF-2DA and flow cytometry analysis. Treatment with **15i** at 50 μM, for 6 h, resulted in a 1.75 fold increase in DAF-2DA fluorescence (GMFC 35.89 ± SEM 3.55) as compared to the vehicle control (GMFC 20.48 ± 6.8). A maximum 3.6-fold (GMFC 74.86 ± 8.9) increase in fluorescence was observed following incubation of the parasite with **15i** for 12 h when compared to the vehicle-treated parasites (Figure 7E). These results indicated that compound **15i**-mediated increase in NO and ROS generation exerts a synergistic effect on leishmanicidal action.

In Vivo Pharmacokinetics Analysis. The mean plasma concentration versus time profiles of **15i** in mice are shown in Figure 8 and the estimated pharmacokinetic parameters were analyzed by WinNonlin software version 8.1 and the results are tabulated in Table 2. After oral administration at 50 mg/kg dose, the maximum attainable concentration (C_{max}) and time taken to attain maximum concentration (T_{max}) were found to be 6860.00 ± 1955.09 ng/mL and 0.75 ± 0.00 h, respectively, which showed that compound **15i** has rapid absorption from the gut. The overall systemic exposure, that is, area under the concentration−time profile ($AUC_{0-\infty}$) of the compound was found to be 18195.95 ± 879.93 h·ng/mL. The apparent volume of distribution (V_d) and Cl were found to be 15.98 ± 1.02 L/Kg and 2.75 ± 0.13 L/h/kg, respectively. However, the time taken for the systemic levels to reduce to half (half-life, $t_{1/2}$) and elimination rate constant (K_e) were found to be 4.02 ± 0.07 h and 0.17 ± 0.003 h^{-1}, respectively. The above-mentioned pharmacokinetic results confirmed that compound **15i** has satisfactory oral exposure and hence may be considered for future optimization as a lead molecule.

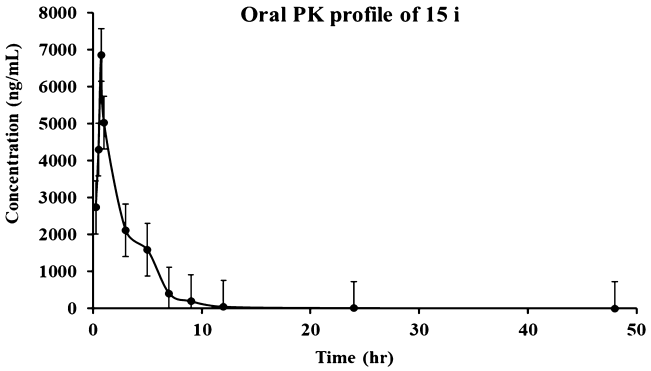

Figure 8. Mean plasma concentrations vs time profile of compound **15i** in BALB/c mice at 50 mg/kg dose.

Table 2. Oral Pharmacokinetics Parameters of CDRI Compound 15i at 50 mg/kg Dose in Mice

parameters	compound **15i**
K_e (h^{-1})	0.17 ± 0.003
$t_{1/2}$ (h)	4.02 ± 0.07
T_{max} (h)	0.75 ± 0.00
C_{max} (ng/mL)	6860.00 ± 1955.09
AUC_{0-48} (h·ng/mL)	18189.18 ± 880.21
$AUC_{0-\infty}$ (h·ng/mL)	18195.95 ± 879.93
V_d (L/kg)	15.98 ± 1.02
Cl (L/h/kg)	2.75 ± 0.13

DOI: 10.1021/acs.jmedchem.9b00628
J. Med. Chem. XXXX, XXX, XXX−XXX

CONCLUSIONS

Current chemotherapeutic interventions against VL demand more novel and safer drugs including patient compliances. Moreover, it should also overcome the barrier of drug resistance against leishmanial strain, as it is a new challenge, which is considered seriously by the scientific community. To throw light on this scenario, the concept of hybridization has been introduced where two or more pharmacophores are brought together in a single entity with individual intrinsic pharmacological activity. This strategy has been already implemented with great success in the discovery of potential leads in diseases like cancer[41] and AIDS[42] and efforts against VLs are currently underway. Recently, triclosan−caffeic acid hybrids were seen to have good antileishmanial activity against *L. (V.) panamensis*.[43] Hybrids of diselenide and sulfonamide also exhibit enhanced antileishmanial activity as compared to their parent components.[44] Hence, in search of new potential candidates, we took the initiative to bring together the pharmacores of quinoline and metranidazole within a single entity. This is because metronidazoles are broad spectrum antiprotozoan drugs, which are known to exert significant efficacy against experimental VL and have the potential to lower parasitic burden if used in combination with other compounds.[45−49] On other hand, quinolines and its derivatives have been reported for their activity against both in vitro and in vivo form of experimental visceral and cutaneous leishmaniasis (against strains like *L. donovani*, *L. chagasi*, *Leishmania major* etc.) with submicromolar IC_{50} values.[50,51] We have synthesized a series of quinoline−metronidazole hybrids and tested their efficacy against *L. donovani*, the causative agent of VL. Among all synthesized compounds **15b** and **15i** were the most promising candidates as they exhibit greater antileishmanial efficacy along with a good safety index and in vitro pharmacokinetics stability. Nevertheless, in case of the in vivo BALB/c model of VL, **15i** performed way better in clearing parasite burden as compared to **15b**. Moreover, **15i** maintained its in vivo safety index as confirmed by AST and ALT, which is further confirmed by the fact that all infected animal did not show any discomfort or uneasiness during or after therapy. Besides that, the oral pharmacokinetic profile of **15i** was also good as **15i** has a rapid absorption from the gut.

Antileishmanial activity can be attained either by upregulating the host immune response, which is an indirect approach or by directly acting upon the parasitic membrane or intracellular organelles. Several antileishmanial compounds like 18β-glycyrrhetinic acid,[52] Fucoidan,[53] and oleuropein,[54] exhibited leishmanicidal effects against *L. donovani* in vitro, and also minimize the parasite burden in *L. donovani*-infected BALB/c mice by Th1 polarization, while drugs like miltefosine[55] and amphotericin-B[56] induce the apoptotic machinery in the parasite. In order to gain a mechanistic overview of the mode of action of **15i**, we checked several biochemical and cell-biological parameters. In our case, we found that **15i** kills the parasite by initiating an apoptotic cascade rather than acting indirectly through host immunity. Apoptosis was also confirmed by DNA fragmentation as observed by the tunnel assay of **15i**-treated promastigotes, where the membrane of the parasite was intact thereby excluding the possibility of necrosis. Our study is in line with other antileishmanial hybrids such as cycloalka[*b*]thiophene and indoles that induce DNA fragmentation and initiate apoptotic cell death in leishmania.[57] In order to initiate an apoptotic cascade, **15i** enters the parasitic compartment without forming pores and then sequentially disturbs the membrane potential of mitochondria, which is an early event of apoptosis as observed by the failure of J-aggregate formation after JC-1 staining. Loss in MMP by **15i** resulted in the leakage of cytochrome *c* from mitochondria to cytosolic compartment. Our results are in accordance with Antinarelli et al., who previously demonstrated that different quinoline conjugates are known to induce depolarization of the MMP in promastigotes. Several other series of compounds are also known to exert their antileishmanial efficacy by depolarizing MMP, for instance, hybrid of β-carboline−quinazolinone diastereomer leads to apoptosis in *L. donovani* promastigotes by depolarizing the mitochondrial membrane.[58] Antileishmanial hybrid compounds are also known to exert their effect by inducing oxidative stress. For instance, β-carboline−quinazolinone hybrids inhibit *L. donovani* trypanothione reductase activity and induce oxidative stress by generating ROS.[58] Similarly, hybrids of β-carboline and 1,3,5-triazine also induce ROS formation in leishmania.[59] In our study, we also found that **15i** has the ability to impair parasite resistance to oxidative stress by enhancing ROS and NO generation, which is crucial for controlling these kinetoplastid protozoan parasites as their life-cycle phase occurring in the acidified phagolysosome of macrophages. These dual characteristic features are attained because of its pharmacophore as quinoline derivatives exerted their antileishmanial effect by inducing the generation of ROS levels and metronidazole series are known to exhibit generation of reactive nitrogen species, including NO. A clear correlation between in vitro activity, safety index, and in vivo activity in conjunction with favorable pharmacokinetics properties suggest the potential of quinoline−metronidazole derivatives for the future development of specific clinical agents for counteracting leishmaniasis and other neglected parasitic diseases.

EXPERIMENTAL SECTION

Synthetic Methods. Reagents were obtained from commercial sources and used without further purification. Silica gel (100−200 mesh) was used to perform column chromatography. Progress of the chemical reactions was monitored by TLC (silica gel plates with fluorescence F254). Melting points were uncorrected. The ^{1}H and ^{13}C NMR spectra were recorded at 300, 400 MHz, and 75, 100 MHz, respectively, using $CDCl_3$ and DMSO-d_6 as a solvent. All chemical shift values were described in ppm and their multiplicities expressed as: m = multiplet, q = quartet, t = triplet, dd = double doublet, brd = broad doublet, d = doublet, brs = broad singlet, and s = singlet. The ESI-MS spectra were recorded on an ion trap LCQ Advantage Max mass spectrometer (Thermo Electron Corporation) and HRMS spectra were recorded by Q-TOF (Agilent 6520). All the final compounds were >95% pure as determined by the HPLC method.

*General Synthetic Method for Preparing 2-(2-Methyl-5-nitro-imidazol-1-yl)-ethyl Ester Toluene-4-sulfonate (**11**).* A mixture of metronidazole **9** (3.14 g, 20 mmol) and Et_3N (3.0 mL, 22 mmol) was dissolved in CH_2Cl_2 (20 mL). Then, the tosyl chloride **10** (3.83 g, 20.1 mmol) in CH_2Cl_2 (10 mL) was added dropwise at 0 °C. The reaction mixture was stirred at room temperature for 5 h. The progress of the reaction was monitored by TLC. After completion of the reaction, 30 mL of ice water was added to the reaction mixture, layer was separated, and the aqueous layer was extracted with ethyl acetate. The combined organic layers were washed with saturated $NaHCO_3$, dried over anhy. Na_2SO_4, filtered, and concentrated under reduced pressure. Compound **11** was obtained as white crystals, which were used for the next steps without further purification.[25]

*General Synthetic Method for Compound Preparation (**13a**−**13b**).* A solution of 2-(2-methyl-5-nitro-1*H*-imidazol-1-yl) ethyl-4-

DOI: 10.1021/acs.jmedchem.9b00628
J. Med. Chem. XXXX, XXX, XXX−XXX

methylbenzenesulfonate **11** (5 g, 0.0153 mol) and 4-hydroxyacetophenone **12a**/3-hydroxyacetophenone **12b** (2.30 g, 0.0169 mol) in the presence of K_2CO_3 in DMF (50 mL) was stirred at room temperature for 24 h. After the completion of the reaction (monitored by TLC), the reaction mixture was suspended in water (50 mL) and extracted with 3-fold with EtOAc (50 mL). After drying on anhy. Na_2SO_4, the combined organic layers were filtered and concentrated to dryness under reduced pressure to afford corresponding product **13a** 1-(3-(2-(2-methyl-5-nitro-1*H*-imidazol-1-yl)ethoxy)phenyl)-ethanone or **13b** 1-(4-(2-(2-methyl-5-nitro-1*H*-imidazol-1-yl)-ethoxy)phenyl)ethanone as yellow solid in good yield.[26]

*1-(3-(2-(2-Methyl-5-nitro-1H-imidazol-1-yl)ethoxy)phenyl)-ethanone (**13a**).* It was obtained as a pale yellow solid, yield 75%; mp: 130−132 °C; ^{1}H NMR (400 MHz, $CDCl_3$): δ 7.97 (s, 1H), 7.54−7.57 (m, 1H), 7.34−7.40 (m, 2H), 7.00−7.03 (m, 1H), 4.74 (t, J = 4.7 Hz, 2H), 4.38 (t, J = 5.0 Hz, 2H),2.63 (s, 3H), 2.58 (s, 3H); ^{13}C NMR ($CDCl_3$, 100 MHz): δ 197.5, 158.0, 151.7, 138.6, 133.3, 129.9, 122.1, 119.7, 112.7, 66.8, 45.9, 26.7, 14.7. ESIMS (m/z): 290 $[M + H]^+$; HRMS (m/z): calcd for $C_{14}H_{15}N_3O_4$ $[M + H]^+$, 290.1135; found, 290.1134.

*General Synthetic Method for Compound Preparation (**15a**−**15m**).* A mixture containing relevant 2-aminoarylketone (1.0 equiv) and 1-(3-(2-(2-methyl-5-nitro-1*H*-imidazol-1-yl)ethoxy)phenyl)-ethanone**13a**/1-(4-(2-(2-methyl-5-nitro-1*H*-imidazol-1-yl)ethoxy)-phenyl)ethanone **13b** (1.0 equiv) were dissolved in TFA (25 mL) and the solution was heated for 3 h at 120 °C. After the completion of condensation reaction[28] (monitored by TLC), the reaction mixture was allowed to attain room temperature. Then, the reaction mixture was neutralized with 0.4 mL of 10% NaOH, extracted with ethyl acetate, and organic layer was washed with water. Organic layer was then evaporated under vacuum and crude product was purified by silica gel column chromatography to obtain **15a**−**15m**.

*2-(3-(2-(2-Methyl-5-nitro-1H-imidazol-1-yl)ethoxy)phenyl)-4-phenylquinoline (**15a**).* It was obtained as a white solid (85%); mp: 171−173 °C; ^{1}H NMR (DMSO-d_6, 400 MHz): δ 8.28 (d, J = 8.8 Hz, 2H), 8.11 (d, J = 8.1 Hz, 1H), 8.04 (s, 1H), 7.97 (s, 1H), 7.82−7.77 (m, 2H), 7.61−7.53 (m, 6H), 7.04 (d, J = 8.8 Hz, 2H), 4.76−4.74 (m, 2H), 4.44−4.42 (m, 2H), 2.56 (s, 3H); ^{13}C NMR (DMSO-d_6, 100 MHz): δ 159.1, 155.1, 151.7, 148.4, 148.0, 138.5, 137.5, 132.8, 131.4, 129.6, 129.4, 128.7, 128.6, 128.4, 126.3, 125.1, 124.7, 118.2, 114.5, 66.4, 45.2, 14.1; ESIMS (m/z): 451 $[M + H]^+$; HRMS (m/z): calcd for $C_{27}H_{22}N_4O_3$ $[M + H]^+$, 451.1770; found, 451.1759.

*4-Methyl-2-(3-(2-(2-methyl-5-nitro-1H-imidazol-1-yl)ethoxy)-phenyl)quinoline (**15b**).* It was obtained as a white solid (69%); mp: 156−158 °C; ^{1}H NMR ($CDCl_3$, 400 MHz): δ 8.17 (d, J = 7.0 Hz, 1H), 8.00−7.98 (m, 2H), 7.74−7.66 (m, 4H), 7.57−7.54 (m, 1H), 7.41−7.38 (m, 1H), 6.90 (d, J = 6.4 Hz, 1H), 4.76−4.75 (m, 2H), 4.46−4.45 (m, 2H), 2.77 (s, 3H), 2.66 (s, 3H); ^{13}C NMR ($CDCl_3$, 100 MHz): δ 158.3, 156.3, 151.9, 148.0, 145.0, 141.6, 138.4, 133.4, 130.3, 130.0, 129.5, 127.4, 126.3, 123.7, 120.9, 119.7, 115.6, 112.9, 66.8, 46.1, 19.0, 14.8; ESIMS (m/z): 389 $[M + H]^+$; HRMS (m/z): calcd for $C_{22}H_{20}N_4O_3$ $[M + H]^+$, 389.1614; found, 389.1597.

*6-Chloro-2-(3-(2-(2-methyl-5-nitro-1H-imidazol-1-yl)ethoxy)-phenyl)-4-phenylquinoline (**15c**).* It was obtained as a white solid (73%); mp: 189−191 °C; ^{1}H NMR ($CDCl_3$, 400 MHz): δ 8.14−8.10 (m, 3H), 7.98 (s, 1H), 7.83−7.82 (m, 1H), 7.75 (s, 1H), 7.65−7.62 (m, 1H), 7.57−7.51 (m, 5H), 6.95−6.93 (m, 2H), 4.76−4.73 (m, 2H), 4.42−4.39 (m, 2H), 2.64 (s, 3H); ^{13}C NMR ($CDCl_3$, 100 MHz): δ 159.1, 156.2, 151.8, 148.5, 147.2, 138.4, 137.8, 133.4, 132.7, 132.0, 131.5, 130.5, 129.4, 129.1, 128.9, 128.8, 126.3, 124.5, 119.5, 114.6, 66.8, 46.0, 14.7; ESIMS (m/z): 485 $[M + H]^+$; HRMS (m/z): calcd for $C_{27}H_{21}ClN_4O_3$ $[M + H]^+$, 485.1380; found, 485.1376.

*6-Bromo-2-(3-(2-(2-methyl-5-nitro-1H-imidazol-1-yl)ethoxy)-phenyl)-4-phenylquinoline (**15d**).* It was obtained as a yellow solid (84%); mp: 103−105 °C; ^{1}H NMR (DMSO-d_6, 400 MHz): δ 8.28 (d, J = 8.8 Hz, 2H), 8.12−8.10 (m, 1H), 8.04 (s, 1H), 7.98 (s, 1H), 7.80−7.76 (m, 4H), 7.60−7.52 (m, 3H), 7.05 (d, J = 8.8 Hz, 2H), 4.77−4.74 (m, 2H), 4.44−4.42 (m, 2H), 2.56 (s, 3H); ^{13}C NMR (DMSO-d_6, 100 MHz): δ 159.2, 155.2, 151.8, 148.0, 147.2, 138.5, 136.7, 132.9, 131.7, 131.6, 131.3, 129.9, 129.5, 128.8, 126.6, 125.0, 124.5, 122.1, 118.3, 114.6, 66.5, 45.2, 14.1; ESIMS (m/z): 529 $[M + H]^+$; HRMS (m/z): calcd for $C_{27}H_{21}BrN_4O_3$ $[M + H]^+$, 529.0875; found, 529.0868.

*2-(3-(2-(2-Methyl-5-nitro-1H-imidazol-1-yl)ethoxy)phenyl)-6-nitro-4-phenylquinoline (**15e**).* It was obtained as a white solid (89%); mp: 229−231 °C; ^{1}H NMR ($CDCl_3$, 400 MHz): δ 8.84−8.83 (m, 1H), 8.50−8.47 (m, 1H), 8.35−7.33 (m, 1H), 7.97 (s, 1H), 7.91 (s, 1H), 7.78−7.74 (m, 2H), 7.62−7.54 (m, 5H), 7.45−7.41 (m, 1H), 6.99−6.96 (m, 1H), 4.79−4.77 (m, 2H), 4.49−4.46 (m, 2H), 2.67 (s, 3H); ^{13}C NMR (DMSO-d_6, 100 MHz): δ 158.7, 158.3, 151.8, 150.7, 150.1, 145.0, 139.1, 138.5, 136.2, 132.9, 131.5, 130.1, 129.7, 129.3, 129.0, 124.2, 123.1, 122.3, 120.8, 120.5, 117.2, 112.9, 66.5, 45.2, 14.2; ESIMS (m/z): 496 $[M + H]^+$; HRMS (m/z): calcd for $C_{27}H_{21}N_5O_5$ $[M + H]^+$, 496.1621; found, 496.1595.

*6-Chloro-4-(2-chlorophenyl)-2-(3-(2-(2-methyl-5-nitro-1H-imidazol-1-yl)ethoxy)phenyl)quinoline (**15f**).* It was obtained as a white solid (88%); mp: 192−194 °C; ^{1}H NMR ($CDCl_3$, 400 MHz): δ 8.18 (d, J = 7.2 Hz, 1H), 7.97 (s, 1H), 7.76 (s, 1H), 7.72−7.66 (m, 3H), 7.60 (d, J = 6.2 Hz, 1H), 7.50−7.37 (m, 5H), 6.93−6.91 (m, 1H), 4.78−4.76 (m, 2H), 4.47−4.45 (m, 2H), 2.66 (s, 3H); ^{13}C NMR ($CDCl_3$, 100 MHz): δ 158.5, 156.3, 151.9, 146.9, 146.0, 140.8, 138.5, 136.3, 133.4, 133.3, 132.7, 131.8, 131.4, 130.8, 130.3, 130.2, 127.1, 126.7, 124.5, 121.0, 120.6, 116.1, 112.9, 66.9, 46.1, 14.9; ESIMS (m/z): 519 $[M + H]^+$; HRMS (m/z): calcd for $C_{27}H_{20}Cl_2N_4O_3$ $[M + H]^+$, 519.0991; found, 519.0976.

*6-Chloro-4-(2-fluorophenyl)-2-(3-(2-(2-methyl-5-nitro-1H-imidazol-1-yl)ethoxy)phenyl)quinoline (**15g**).* It was obtained as a white solid (79%); mp: 202−204 °C; ^{1}H NMR ($CDCl_3$, 400 MHz): δ 8.18 (d, J = 7.1 Hz, 1H), 7.97 (s, 1H), 7.80 (s, 1H), 7.71−7.67 (m, 3H), 7.62 (s, 1H), 7.54−7.52 (m, 1H), 7.44−7.38 (m, 2H), 7.36−7.33 (m, 1H), 7.31−7.27 (m, 1H), 6.93−6.92 (m, 1H), 4.77−4.75 (m, 2H), 4.47−4.43 (m, 2H), 2.65 (s, 3H); ^{13}C NMR ($CDCl_3$, 100 MHz): δ 160.9, 158.5, 156.3, 151.9, 147.0, 142.8, 140.8, 133.5, 132.7, 131.8, 131.7, 131.7, 131.1, 131.0, 130.8, 130.2, 126.8, 125.2, 125.0, 124.7, 124.6, 124.4, 121.0, 120.9, 116.5, 116.3, 116.1, 112.9, 66.94, 46.2, 14.9; ESIMS (m/z): 503 $[M + H]^+$; HRMS (m/z): calcd for $C_{27}H_{20}ClFN_4O_3$ $[M + H]^+$ 503.1286; found, 503.1284.

*2-(4-(2-(2-Methyl-5-nitro-1H-imidazol-1-yl)ethoxy)phenyl)-4-phenylquinoline (**15h**).* It was obtained as a white solid (84%); mp: 141−143 °C; ^{1}H NMR ($CDCl_3$, 400 MHz): δ 8.19 (d, J = 8.0 Hz, 3H), 8.15−8.13 (m, 1H), 7.98−7.86 (m, 1H), 7.74−7.71 (m, 2H), 7.55−7.50 (m, 5H), 7.47−7.44 (m, 1H), 6.95−6.93 (m, 2H), 4.76−4.73 (m, 2H), 4.42−4.39 (m, 2H), 2.62 (s, 3H); ^{13}C NMR ($CDCl_3$, 100 MHz): δ 158.9, 156.0, 151.8, 149.2, 148.8, 138.5, 133.4, 133.2, 129.9, 129.6, 129.1, 128.6, 128.5, 126.2, 125.7, 125.6, 118.8, 114.6, 66.8, 46.0, 14.8; ESIMS (m/z): 451 $[M + H]^+$; HRMS (m/z): calcd for $C_{27}H_{22}N_4O_3$ $[M + H]^+$, 451.1770; found, 451.1763.

*4-Methyl-2-(4-(2-(2-methyl-5-nitro-1H-imidazol-1-yl)ethoxy)-phenyl)quinoline (**15i**).* It was obtained as a white solid (78%); mp: 124−126 °C; ^{1}H NMR ($CDCl_3$, 400 MHz): δ 8.13−8.08 (m, 3H), 7.98−7.95 (m, 2H), 7.71−7.67 (m, 1H), 7.64 (s, 1H), 7.53−7.49 (m, 1H), 6.93 (d, J = 8.8 Hz, 2H), 4.74−4.72 (m, 2H), 4.40−4.38 (m, 2H), 2.74 (s, 3H), 2.63 (s, 3H); ^{13}C NMR (DMSO-d_6, 100 MHz): δ 158.9, 155.1, 151.7, 147.3, 144.9, 138.5, 132.8, 131.6, 129.4, 129.3, 128.5, 126.6, 125.8, 123.9, 118.6, 114.5, 66.4, 45.2, 18.3, 14.1; ESIMS (m/z): 389 $[M + H]^+$; HRMS (m/z): calcd for $C_{22}H_{20}N_4O_3$ $[M + H]^+$, 389.1614; found, 389.1605.

*6-Chloro-2-(4-(2-(2-methyl-5-nitro-1H-imidazol-1-yl)ethoxy)-phenyl)-4-phenylquinoline (**15j**).* It was obtained as a yellow solid (83%); mp: 196−198 °C; ^{1}H NMR (DMSO-d_6, 400 MHz): δ 8.29 (d, J = 8.8 Hz, 2H), 8.13 (d, J = 8.9 Hz, 1H), 8.04 (s, 2H), 7.80−7.77 (m, 1H), 7.72 (s, 1H), 7.63−7.57 (m, 5H), 7.05 (d, J = 8.5 Hz, 2H), 4.76−4.74 (m, 2H), 4.45−4.42 (m, 2H), 2.55 (s, 3H); ^{13}C NMR ($CDCl_3$, 100 MHz): δ 159.2, 156.2, 151.8, 148.5, 147.3, 137.8, 133.5, 132.9, 132.0, 131.6, 130.5, 129.5, 129.1, 128.9, 128.8, 126.4, 124.6, 119.5, 114.6, 66.9, 46.1, 14.8; ESIMS (m/z): 485 $[M + H]^+$; HRMS (m/z): calcd for $C_{27}H_{21}ClN_4O_3$ $[M + H]^+$, 485.1380; found, 485.1370.

*7-Bromo-2-(4-(2-(2-methyl-5-nitro-1H-imidazol-1-yl)ethoxy)-phenyl)-4-Phenylquinoline (**15k**).* It was obtained as a white solid

DOI: 10.1021/acs.jmedchem.9b00628
J. Med. Chem. XXXX, XXX, XXX−XXX

(71%); mp: 153−155 °C; ^{1}H NMR ($CDCl_3$, 400 MHz): δ 8.19 (d, J = 8.4 Hz, 1H), 8.12 (d, J = 8.7 Hz, 2H), 7.97 (s, 1H), 7.80 (d, J = 8.2 Hz, 1H), 7.73−7.66 (m, 4H), 7.47−7.40 (m, 3H), 6. 49 (d, J = 8.7 Hz, 2H), 4.75−4.73 (m, 2H), 4.41−4.39 (m, 2H), 2.64 (s, 3H); ^{13}C NMR ($CDCl_3$, 100 MHz): δ 158.9, 155.9, 151.7, 148.7, 147.8, 138.4, 137.2, 133.3, 132.9, 131.8, 131.1, 130.0, 129.7, 129.0, 126.3, 125.2, 122.8, 118.6, 114.5, 66.7, 45.9, 14.7; ESIMS (m/z): 529 $[M + H]^+$; HRMS (m/z): calcd for $C_{27}H_{21}BrN_4O_3$ $[M + H]^+$, 529.0875; found, 529.0870.

*6-Chloro-4-(2-chlorophenyl)-2-(4-(2-(2-methyl-5-nitro-1H-imidazol-1-yl)ethoxy)phenyl)quinoline (**15l**).* It was obtained as a white solid (78%); mp: 217−219 °C; ^{1}H NMR ($CDCl_3$, 400 MHz): δ 8.12 (d, J = 8.8 Hz, 3H), 7.98 (s, 1H), 7.78 (s, 1H), 7.66−7.63 (m, 1H), 7.60−7.55 (m, 1H), 7.54−7.49 (m, 1H), 7.44−7.40 (m, 1H), 7.35−7.33 (m, 1H), 7.31−7.28 (m, 1H), 6.94 (d, J = 8.8 Hz, 2H), 4.75−4.73 (m, 2H), 4.41−4.39 (m, 2H), 2.64 (s, 3H); ^{13}C NMR ($CDCl_3$, 100 MHz): δ 160.9, 159.2, 158.4, 156.2, 151.8, 147.0, 142.6, 138.5, 133.4, 132.6, 132.2, 131.7, 131.6, 131.5, 131.0, 130.9, 130.7, 129.1, 126.5, 125.2, 125.1, 124.6, 124.4, 120.5, 116.4, 116.2, 114.6, 66.8, 46.0, 14.8; ESIMS (m/z): 519 $[M + H]^+$; HRMS (m/z): calcd for $C_{27}H_{20}Cl_2N_4O_3$ $[M + H]^+$, 519.0991; found, 519.0978.

*6-Chloro-4-(2-fluorophenyl)-2-(4-(2-(2-methyl-5-nitro-1H-imidazol-1-yl)ethoxy)phenyl)quinoline (**15m**).* It was obtained as a yellow solid (88%); mp: 204−206 °C; ^{1}H NMR ($CDCl_3$, 400 MHz): δ 8.14−8.11 (m, 3H), 7.98 (s, 1H), 7.74 (s, 1H), 7.65−7.63 (m, 1H), 7.59 (d, J = 6.3 Hz, 1H), 7.49−7.43 (m, 3H), 7.37−7.36 (m, 1H), 6.94 (d, J = 7.0 Hz, 2H), 4.76−4.74 (m, 2H), 4.42−4.40 (m, 2H), 2.64 (s, 3H); ^{13}C NMR ($CDCl_3$, 100 MHz): δ 159.2, 156.1, 151.8, 146.9, 145.8, 138.5, 136.3, 133.4, 133.3, 132.6, 132.1, 131.5, 131.4, 130.6, 130.2, 130.1, 129.1, 127.1, 126.4, 124.4, 120.0, 114.6, 66.8, 40.6, 14.8; ESIMS (m/z): 503 $[M + H]^+$; HRMS (m/z): calcd for $C_{27}H_{20}ClFN_4O_3$ $[M + H]^+$, 503.1286; found, 503.1284.

Biological Assays. *Maintenance of Cell Line and Parasite Culture.* Luciferase expressing *L. donovani* promastigotes strain (MHOM/IN/80/Dd8) was obtained as described elsewhere.[60] Briefly, the firefly luciferase gene (complete ORF) was amplified from pGEM-Luc plasmid DNA (Promega) and cloned in the pCRII-TOPO vector. The purified insert was obtained after digestion with the restriction enzyme SpeI and subsequently cloned into dephosphorylated pKS-Neo leishmania shuttle vector containing neomycin cascade to generate the pKS-Neo-luc construct. The orientation of the luc insert was confirmed after double digestion with restriction enzymes, that is, EcoRI and BamHI and selected in *Escherichia coli* before carrying out transfection. *L. donovani* promastigotes were transfected with pKS-Neo-luc construct by electroporation with a Gene Pulser (Bio-Rad) and the transfected parasites were cultured in M199 medium which was supplemented with 10% heat-inactivated fetal bovine serum (FBS) and G418 disulphate (20 μg/mL) at 24 °C. J774 macrophages cell line was maintained in complete RPMI medium as described previously.[61]

Luciferase and MTT Assay. In vitro antileishmanial activity of quinoline−metronidazole derivatives was assessed by luciferase assay using *Leishmania* parasite (MHOM/IN/80/Dd8 constitutively expressing firefly luciferase gene). Parasite multiplication was represented as relative luminescence unit (RLU) and the IC_{50} value of the synthesized derivatives and standard drugs was determined as described earlier.[61] Antipromastigote activity of **15b** and **15i** was also assessed at various concentrations by MTT assay as described elsewhere.[62] The absorbance was recorded on a microplate spectrophotometer (BioTek Instruments, Winooski, VT, USA), and the data were represented as percentage viability of promastigotes in comparison with control cells.

Antiamastigote Assay. Antileishmanial activity of quinoline−metronidazole derivatives against intracellular amastigotes was assessed by luciferase assay at different concentrations as described previously.[61] Parent molecules: metronidazole (Acros Organics, Belgium) and quinoline (Sigma-Aldrich, USA), compounds (**15b** and **15i**), and standard drug miltefosine (Synphabase, Switzerland) were subjected to serial dilution at a 2-fold concentration in RPMI medium, maintaining the final concentrations in a range between 3.125 and 100 μM prior to treatment in infected macrophages. The antiamastigote activity of **15b** and **15i** was also evaluated by Giemsa staining through microscopic counting of the number of amastigotes/100 macrophages.[63]

Mammalian Cell Cytotoxicity Assay. Vero cells and J774 macrophages were selected to assess the cytotoxic effects of **15b** and **15i** at different concentrations (12.5−400 μM) by MTT assay as described previously.[61] The 50% cellular cytotoxic concentration (CC_{50}) and selectivity index (SI) of **15b** and **15i** were determined as described previously.[64]

Animal Infection and Therapeutic Protocol. The *L. donovani* strain MHOM/IN/80/Dd8 was maintained by serial passage in hamsters for the establishment of infection. Amastigotes were then isolated from the spleen of *L. donovani*-infected golden hamsters (2 months) and transformation into the promastigote form was obtained in M199 (pH 7.4) medium, enriched with 20% FBS (heat-inactivated), 25 mM HEPES, 2 mM glutamine, 100 μg/mL streptomycin, and 100 IU/mL penicillin. After serial passages for 2 times, stationary-phase promastigotes were collected from the culture medium and injected in BALB/c mice through the tail vein [2×10^7/0.2 mL of phosphate-buffered saline (PBS)] to establish infection. The level of infection was determined by performing autopsy in the liver and spleen of 3−4 mice selected randomly at day 15 postinfection. Animals with similar levels of the organ parasitic load were further selected for the in vivo experiment. Treatment was initialized intraperitoneally (ip) for **15b** and **15i** and miltefosine was administered orally in 15 day infected BALB/c mice. Five animals/groups were used for the study and the groups were as follows: infected untreated, infected vehicle-treated (8% DMSO in PBS), infected miltefosine (a standard antileishmanial drug)-treated, infected quinoline-treated, infected metronidazole-treated, infected **15b**-treated, and infected **15i**-treated. Miltefosine (25 mg/kg) was suspended in triple distilled water and given orally, while **15b** and **15i** were dissolved in DMSO (8%). Animals were administered with **15b** and **15i** via intraperitoneal route for 5 consecutive days, and sacrificed at day 7 post-treatment, following which the liver and spleen parasite burden were assessed by Giemsa staining and expressed as LDU.[61]

Ethics Statement for in Vivo Experiments. All in vivo animal experiments were conducted as per the strict guidelines and recommendations provided by the specialized Committee for the Purpose of Control and Supervision of Experiments on Animals (CPCSEA), New Delhi, India. Animals usage was officially permitted by the IAEC (Institutional Animal Ethical Committee) and all in vivo experiments were performed in agreement with the IAEC of the CSIR-CDRI (IAEC approval no: IAEC/2017/190). BALB/c mice of weight 20 ± 2 g were procured from the National Laboratory Animal Center, CSIR-CDRI (Lucknow, India) and maintained in suitable experimental conditions such as room temperature (24 ± 2 °C) and 40−60% relative humidity while on a regular 12 h light−dark cycle. The animals were acclimatized for a minimum period of 3 days prior to the experiment.

Th1/Th2 Cytokine Estimation. The levels of Th1/Th2 cytokines in the cell culture supernatants of **15i**-treated infected macrophages was assessed using ELISA kit (BD Biosciences, USA) as described elsewhere.[61]

Detection of Plasma Membrane Permeability. Plasma membrane integrity was determined using the Sytox green dye as mentioned elsewhere[65] with some modifications. Briefly, promastigotes [4×10^6/mL) were incubated with 50 μM **15i** for 0−360 min. This was followed by washing with PBS for two times and incubation with 2 μM Sytox green at 28 °C for 15 min. The promastigotes were then collected in fluorescence-activated cell sorting (FACS) tubes and the fluorescence emitted upon binding of the dye to intracellular nucleic acids was recorded by flow cytometry (BD FACSCalibur platform, with excitation and emission wavelengths at 485 and 535 nm, respectively). 0.1% Triton X-100 was used to obtain maximal promastigote permeabilization and data were represented with respect to the fluorescence obtained in this sample.

Apoptosis Detection by Annexin V/PI Staining. Phosphatidylserine externalization in vehicle or **15i**-treated *L. donovani* promastigotes

DOI: 10.1021/acs.jmedchem.9b00628
J. Med. Chem. XXXX, XXX, XXX−XXX

(12−48 h) was determined by using the Apoptosis Detection Kit (Sigma-Aldrich, USA) as described previously.[61] Analysis of stained promastigotes was performed in BD FACSCalibur platform and CellQuest software was used for data interpretation.

TUNEL Assay. Fragmentation of DNA within the *L. donovani* parasite was analyzed by terminal deoxynucleotidyltranferase (TdT)-mediated dUTP nick end labeling (TUNEL) using APO BrdU TUNEL Assay Kit (Molecular Probes, USA) as per the manufacturer's instructions. Briefly, 1×10^5 parasites were harvested after treatment with 50 μM **15i** for 48 h and samples treated with DMSO (0.1%) were then used as the vehicle control. The experiment was performed as described previously.[66] Samples were finally observed under a confocal microscope (LSM, Zeiss, Germany) and analyzed on adobe Photoshop software 7.

Determination of Metacaspase-Like Protease Activity. Metacaspase activity was determined by using the substrate, BOC-GRR-AMC. Briefly, 5×10^6 exponential phase parasites were either untreated or incubated with DMSO (0.1%), **15i** (50 μM) either alone or in parasites pretreated with antipain (1 μM), zVAD-fmk (z-Val-Ala-Asp-fmk) (100 μM) for 1 h. The cells were then pulled, subjected to lysis in cell lysis buffer and resuspended in metacaspase buffer to detect metacaspase activities. Furthermore, cell lysates were then subjected to 100 μM fluorogenic substrate BOC-GRR-AMC and 1× reaction buffer supplemented with 100 μM dithiothreitol. Samples were then incubated at 37 °C for 2 h and the released 7-amino-4-methylcoumarin (AMC) was detected by fluorometry (BMG POLARstar Galaxy, Virginia, USA), with excitation and emission wavelengths at 380 and 460 nm, respectively. The results were represented as relative fluorescence units and normalized with cellular protein extracts in mg.

Measurement of MMP Change. Change in MMP ($\Delta\Psi_m$) in **15i**-treated promastigotes (6−48 h) was evaluated using JC-1 dye (MitoProbe JC-1 Assay Kit, Molecular Probes, USA) as described previously.[61] The experimental data were recorded in BD FACSCalibur platform and analyzed by CellQuest Software.

Cytochrome c Detection in the Mitochondrial and Cytosolic Fraction of L. donovani. Mitochondria fractions were obtained from untreated and **15i**-treated *L. donovani* promastigotes using the ApoAlert cell fractionation kit (Takara, Japan) as per the manufacturer's instructions, and stored at −20 °C at a final protein concentration of 7−8 mg/mL. Cytosolic lysates of control and **15i**-treated promastigotes were prepared as described elsewhere.[66] After cell fractionation, mitochondrial and cytosolic levels of cytochrome *c* were determined by immunoblot as described previously.[66]

Determination of ATP Generation. Promastigotes (2×10^6) were treated with 50 μM **15i** for varying time periods, and the amount of ATP content was evaluated by using the luciferase ATP assay kit (Invitrogen, Inc., Ltd. USA), as described previously.[67]

ROS Measurement. Promastigotes (2×10^6 cells/mL) were incubated with 50 μM **15i** for different time points (12−48 h) and DMSO (0.1%)-treated parasites were used as the vehicle control. Parasites were then harvested, followed by resuspension in PBS. Thereafter, 20 μM (DCFDA) was added to the parasites and incubation was performed for 20 min in the dark at 37 °C.[34] Thereafter, analysis was performed on BD FACSCalibur platform at 530 nm wavelength.

NO Measurement. Promastigotes (2×10^6 cells/mL) were incubated with 50 μM **15i** for different time points (6−18 h) and DMSO (0.1%)-treated parasites were used as the vehicle control. Promastigotes were finally collected, followed by resuspension in PBS, and incubated with 40 μM of DAF-2DA at 37 °C for 45 min in the dark. The resultant fluorescence was measured and analyzed on BD FACSCalibur platform.

UPLC Conditions for in Vitro PK Study. Compounds **15b** and **15i** were analyzed on Shimadzu UPLC system equipped with the photodiode array detector. Chromatographic separation of both compounds was achieved with a mobile phase composition of acetonitrile: formic acid (0.1%) on a C18 column (100 × 4.6 mm, 5.0 μm). The mobile phase ratio for compound **15b** and **15i** were optimized as 50:50 (v/v) and 40:60 (v/v), respectively. The flow rates for elution of compound **15b** and **15i** were set as 1.0 and 0.8 mL/min, respectively.

In Vitro SGF and SIF Stability. SGF and SIF were prepared as per USP specifications.[68] The stability studies of compound **15b** and **15i** in SGF and SIF were performed at 10 μg/mL in triplicate. Briefly, SGF and SIF were taken in two separate glass test tubes and preincubated in shaking water bath for 10−15 min at 37 ± 2 °C. Afterward, aliquots of **15b** and **15i** were spiked separately in SGF and SIF and 100 μL of the incubation mixture was withdrawn at 0, 5, 10, 15, 30, 45, 60, 90, and 120 min. Each sample was quenched with acetonitrile 1:2 (% v/v), vortexed, and centrifuged for 10 000 rpm. The supernatant was then analyzed by the UPLC system.

In Vitro Plasma Stability. The plasma stability of **15b** and **15i** was performed at 10 μg/mL in triplicate. The blank rat plasma was taken in test tubes and preincubated in shaking water bath for 10 min at 37 ± 0.2 °C. Afterward, aliquots of compound **15b** and **15i** were spiked to incubated plasma and samples were withdrawn at 0, 5, 10, 15, 30, 45, 60, 90, and 120 min. Precipitation was carried out with the addition of acetonitrile in the ratio of 1:2 (v/v) at each time intervals, followed by vortexing and centrifugation for 10 min at 10 000 rpm. Supernatants were separated and subjected for analysis by UPLC.

In Vitro Microsomal Stability. Microsomal stability of **15b** and **15i** was performed from RLM in triplicate. Briefly, in each glass tube, 446.25 μL of Tris buffer (50 mM, pH 7.4), magnesium chloride ($MgCl_2$, 40 μM), and RLM protein (0.5 mg/mL) were spiked and incubated for at 37 ± 0.2 °C for 5 min. Then, compounds **15b** and **15i** (10 μg/mL) were spiked separately in this preincubation mixture. Positive and negative controls were also performed in RLM for validation of assays and microsomal activity. Initiation of the reaction was performed by adding NADPH (24 mM) followed by incubation for 1 h. The reaction was terminated by adding ice-chilled acetonitrile (100 μL) to the reaction mixture (50 μL) collected at predefined time points (0, 5, 10, 15, 30, 45, and 60 min). Samples were vortex mixed for 5 min, followed by centrifugation for 10 min at 10 000 rpm. The 20 μL of supernatant was directly analyzed by UPLC.

Data Analysis. The percentage of compound remaining intact at different time intervals after incubation was determined by the eq 1 and the in vitro metabolic half-life ($t_{1/2}$) was determined by plotting the natural logarithm of percentage compound remaining versus time.[69,70] The slope of the curve was represented as depletion rate constant K (min^{-1}). The half-life of metabolic stability was estimated using the first-order eq 2. The in vitro intrinsic clearance (CL_{int}) was calculated through the eq 3.

$$\%\ \text{Drug remaining} = \frac{\text{concentration of drug after incubation}}{\text{concentration of drug before incubation}} \times 100 \quad (1)$$

$$\text{Half-life } (t_{1/2}) = \frac{0.693}{K} \quad (2)$$

$$\text{Intrinsic clearance } CL_{int} = K \times \frac{\text{volume of incubation } (\mu L)}{\text{amount of protein incubated (mg)}} \quad (3)$$

where K represents the depletion rate constant and it was calculated from the slope of linear regression from natural log percentage of the substrate remaining versus incubation time.

In Vivo Pharmacokinetic Study. In vivo oral PK study of compound **15i** was performed in BALB/c male mice (n = 5). The compound was administered at 50 mg/kg dose via oral gavage to each mice and the oral suspension was formulated in (0.25% CMC solution and 5% Tween 80). Blood samples were collected from the retro-orbital plexus of mice under light ether anesthesia into heparin-containing microfuge tubes at 0.25, 0.5, 1, 3, 5, 7, 9, 12, 24, and 48 h of postdose. Plasma was harvested by centrifugation of blood at 10 000 rpm for 10 min and stored at −20 ± 2 °C until bioanalysis. The protein precipitation method was employed for sample processing by using acetonitrile (200 μL/100 μL plasma) as protein precipitant

DOI: 10.1021/acs.jmedchem.9b00628
J. Med. Chem. XXXX, XXX, XXX−XXX

containing medicarpin as internal standard. The supernatant was injected for LC-MS/MS.

Statistical Analysis. Data are represented as the mean ± SD of three separate experiments. To calculate the statistical significance between the groups under study, we used the software GraphPad Prism (version 5) and the differences between the experimental sets were analyzed by one-way ANOVA followed by Tukey's post. $P < 0.05$ was considered statistically significant.

■ ASSOCIATED CONTENT

Supporting Information

The Supporting Information is available free of charge on the ACS Publications website at DOI: 10.1021/acs.jmedchem.9b00628.

SMILES strings (CSV)

^{1}H NMR and ^{13}C NMR spectra of all compounds (PDF)

■ AUTHOR INFORMATION

Corresponding Authors

*E-mail: kv_sashidhara@cdri.res.in. Phone: +91-522-2772450, ext. 4683/4684. Fax: +91-522-2771942/2771970 (K.V.S.).

*E-mail: susantakar@cdri.res.in. Phone: +91-522-2772450, ext. 4495 (S.K.).

ORCID

Susanta Kar: 0000-0002-9907-539X

Author Contributions

⊥A.U and P.C. contributed equally to this work.

Notes

The authors declare no competing financial interest.

■ ACKNOWLEDGMENTS

This study was funded by the Department of Science and Technology (grant no. SB/FT/LS-310/2012), Council of Scientific and Industrial Research (CSIR NWP BSC0114). N.P., A.U., P.K., M.R. received fellowship from UGC (New Delhi), P.C., P.V., and S.G., S.K.S. are the recipients of fellowships from CSIR (New Delhi). The transgenic *L. donovani* promastigotes was a kind gift from Dr. Neena Goyal, Division of Biochemistry, CSIR-CDRI, Lucknow, India. The authors are thankful to Anuradha Seth for copy-editing the manuscript. The authors would also like to acknowledge the Director, CSIR-CDRI, Lucknow, for facilitating the research. Authors are also thankful to the sophisticated analytical instrumentation facility of CSIR-CDRI for providing support with the confocal microscopy and flow cytometry experiments. This manuscript has CDRI Communication no. 9845.

■ ABBREVIATIONS

VL, visceral leishmaniasis; MET-OH, metronidazole; ROI, reactive nitrogen species; HAT, human African trypanosomiasis; RNI, reactive nitrogen species; IC_{50}, half-maximal inhibitory concentration; SAR, structure−activity relationship; RLM, rat liver microsomes; MTT, 3-(4,5-dimethylthiazol-2-yl)-2,5-diphenyltetrazolium bromide; ALT, alanine aminotransferase; ip, intraperitoneal; AST, aspartate aminotransferase; MIC, maximum inhibitory concentration; CC_{50}, 50% reduction of viability of treated cells with respect to untreated cells; MMP, mitochondrial membrane potential; SI, selectivity index; ROS, reactive oxygen species; NO, nitric oxide; FITC, fluorescein isothiocyanate; PI, propidium iodide; SGF, simulated gastric fluid; TUNEL, terminal deoxynucleotidyl transferase dUTP nick end labeling; FBS, fetal bovine serum; SIF, simulated intestinal fluid; K, depletion rate constant; CL_{int}, intrinsic clearance; AUC, area under the curve; HPLC, high-performance liquid chromatography; $t_{1/2}$, half-time; HRMS, high-resolution mass spectrometry; C_{max}, maximum concentration; IR, infrared spectroscopy; DMSO, dimethyl sulfoxide; NMR, nuclear magnetic resonance; EtOH, ethanol; CH_3COOH, acetic acid; Cl, clearance; V_d, volume of distribution; TLC, thin-layer chromatography; K_e, elimination rate constant; CH_3CN, acetonitrile; LDU, Leishmania Donovan unit; FACS, fluorescence-activated cell sorting; BOC-GRR-AMC, *t*-butyloxycarbonyl-Gly-Arg-Arg-AMC; zVAD-fmk, z-Val-Ala-Asp-fmk; RLU, relative luminescence unit

■ REFERENCES

(1) Chappuis, F.; Sundar, S.; Hailu, A.; Ghalib, H.; Rijal, S.; Peeling, R. W.; Alvar, J.; Boelaert, M. Visceral leishmaniasis: What are the needs for diagnosis, treatment and control? *Nat. Rev. Microbiol.* **2007**, *5*, 873−882.

(2) Murray, H. W.; Berman, J. D.; Davies, C. R.; Saravia, N. G. Advances in leishmaniasis. *Lancet* **2005**, *366*, 1561−1577.

(3) Desjeux, P. Leishmaniasis: Current situation and new perspectives. *Comp. Immunol. Microbiol. Infect. Dis.* **2004**, *27*, 305−318.

(4) Bhattacharya, S. K.; Sur, D.; Karbwang, J. Childhood visceral leishmaniasis. *Indian J. Med. Res.* **2006**, *123*, 353−356.

(5) Sundar, S. Drug resistance in indian visceral leishmaniasis. *Trop. Med. Int. Health* **2001**, *6*, 849−854.

(6) Freitas-Junior, L. H.; Chatelain, E.; Kim, H. A.; Siqueira-Neto, J. L. Visceral leishmaniasis treatment: What do we have, what do we need and how to deliver it? *Int. J. Parasitol.: Drugs Drug Resist.* **2012**, *2*, 11−19.

(7) Jha, T. K. Drug unresponsiveness & combination therapy for kala-azar. *Indian J. Med. Res.* **2006**, *123*, 389−398.

(8) Sundar, S.; More, D. K.; Singh, M. K.; Singh, V. P.; Sharma, S.; Makharia, A.; Kumar, P. C. K.; Murray, H. W. Failure of pentavalent antimony in visceral leishmaniasis in india: Report from the center of the indian epidemic. *Clin. Infect. Dis.* **2000**, *31*, 1104−1107.

(9) Agrawal, V.; Singh, Z. Miltefosine: First oral drug for treatment of visceral leishmaniasis. *Med. J. Armed Forces India* **2006**, *62*, 66−67.

(10) Soto, J.; Toledo, J.; Gutierrez, P.; Nicholls, R. S.; Padilla, J.; Engel, J.; Fischer, C.; Voss, A.; Berman, J. Treatment of american cutaneous leishmaniasis with miltefosine, an oral agent. *Clin. Infect. Dis.* **2001**, *33*, E57−E61.

(11) Monge-Maillo, B.; López-Vélez, R. Miltefosine for visceral and cutaneous leishmaniasis: drug characteristics and evidence-based treatment recommendations. *Clin. Infect. Dis.* **2015**, *60*, 1398−1404.

(12) Patterson, S.; Wyllie, S.; Stojanovski, L.; Perry, M. R.; Simeons, F. R. C.; Norval, S.; Osuna-Cabello, M.; De Rycker, M.; Read, K. D.; Fairlamb, A. H. TheREnantiomer of the Antitubercular Drug PA-824 as a Potential Oral Treatment for Visceral Leishmaniasis. *Antimicrob. Agents Chemother.* **2013**, *57*, 4699−4706.

(13) Patterson, S.; Wyllie, S.; Norval, S.; Stojanovski, L.; Simeons, F. R. C.; Auer, J. L.; Osuna-Cabello, M.; Read, K. D.; Fairlamb, A. H. The anti-tubercular drug delamanid as a potential oral treatment for visceral leishmaniasis. *eLife* **2016**, *5*, e09744.

(14) Wyllie, S.; Patterson, S.; Stojanovski, L.; Simeons, F. R. C.; Norval, S.; Kime, R.; Read, K. D.; Fairlamb, A. H. The anti-trypanosome drug fexinidazole shows potential for treating visceral leishmaniasis. *Sci. Transl. Med.* **2012**, *4*, 119re1.

(15) Mukkavilli, R.; Pinjari, J.; Patel, B.; Sengottuvelan, S.; Mondal, S.; Gadekar, A.; Verma, M.; Patel, J.; Pothuri, L.; Chandrashekar, G.; Koiram, P.; Harisudhan, T.; Moinuddin, A.; Launay, D.; Vachharajani, N.; Ramanathan, V.; Martin, D. In vitro metabolism, disposition, preclinical pharmacokinetics and prediction of human pharmacoki-

DOI: 10.1021/acs.jmedchem.9b00628
J. Med. Chem. XXXX, XXX, XXX−XXX

netics of dndi-vl-2098, a potential oral treatment for visceral leishmaniasis. *Eur. J. Pharm. Sci.* **2014**, *65*, 147−155.
(16) Wyllie, S.; Roberts, A. J.; Norval, S.; Patterson, S.; Foth, B. J.; Berriman, M.; Read, K. D.; Fairlamb, A. H. Activation of bicyclic nitro-drugs by a novel nitroreductase (ntr2) in leishmania. *PLoS Pathog.* **2016**, *12*, e1005971.
(17) Bongarzone, S.; Bolognesi, M. L. The concept of privileged structures in rational drug design: Focus on acridine and quinoline scaffolds in neurodegenerative and protozoan diseases. *Expert Opin. Drug Discovery* **2011**, *6*, 251−268.
(18) Keri, R. S.; Patil, S. A. Quinoline: A promising antitubercular target. *Biomed. Pharmacother.* **2014**, *68*, 1161−1175.
(19) Solomon, V. R.; Lee, H. Quinoline as a privileged scaffold in cancer drug discovery. *Curr. Med. Chem.* **2011**, *18*, 1488−1508.
(20) Vlahopoulos, S.; Critselis, E.; Voutsas, I.; Perez, S.; Moschovi, M.; Baxevanis, C.; Chrousos, G. New use for old drugs? Prospective targets of chloroquines in cancer therapy. *Curr. Drug Targets* **2014**, *15*, 843−851.
(21) Loiseau, P. M.; Cojean, S.; Schrével, J. Sitamaquine as a putative antileishmanial drug candidate: From the mechanism of action to the risk of drug resistance. *Parasite* **2011**, *18*, 115−119.
(22) Carvalho, L.; Luque-Ortega, J. R.; Manzano, J. I.; Castanys, S.; Rivas, L.; Gamarro, F. Tafenoquine, an antiplasmodial 8-aminoquinoline, targets leishmania respiratory complex iii and induces apoptosis. *Antimicrob. Agents Chemother.* **2010**, *54*, 5344−5351.
(23) Antinarelli, L. M. R.; Dias, R. M. P.; Souza, I. O.; Lima, W. P.; Gameiro, J.; da Silva, A. D.; Coimbra, E. S. 4-aminoquinoline derivatives as potential antileishmanial agents. *Chem. Biol. Drug Des.* **2015**, *86*, 704−714.
(24) Coimbra, E. S.; Antinarelli, L. M. R.; Silva, N. P.; Souza, I. O.; Meinel, R. S.; Rocha, M. N.; Soares, R. P. P.; da Silva, A. D. Quinoline derivatives: Synthesis, leishmanicidal activity and involvement of mitochondrial oxidative stress as mechanism of action. *Chem.-Biol. Interact.* **2016**, *260*, 50−57.
(25) Mao, W.-J.; Lv, P.-C.; Shi, L.; Li, H.-Q.; Zhu, H.-L. Synthesis, molecular docking and biological evaluation of metronidazole derivatives as potent helicobacter pylori urease inhibitors. *Bioorg. Med. Chem.* **2009**, *17*, 7531−7536.
(26) Anthwal, A.; Rajesh, U. C.; Rawat, M. S. M.; Kushwaha, B.; Maikhuri, J. P.; Sharma, V. L.; Gupta, G.; Rawat, D. S. Novel metronidazole-chalcone conjugates with potential to counter drug resistance in trichomonas vaginalis. *Eur. J. Med. Chem.* **2014**, *79*, 89−94.
(27) Marco-Contelles, J.; Pérez-Mayoral, E.; Samadi, A.; do Carmo Carreiras, M.; Soriano, E. Recent Advances in the Friedländer Reaction. *Chem. Rev.* **2009**, *109*, 2652−2671.
(28) Shaabani, A.; Soleimani, E.; Badri, Z. Triflouroacetic acid as an efficient catalyst for the synthesis of quinoline. *Synth. Commun.* **2007**, *37*, 629−635.
(29) Zalila, H.; González, I. J.; El-Fadili, A. K.; Delgado, M. B.; Desponds, C.; Schaff, C.; Fasel, N. Processing of metacaspase into a cytoplasmic catalytic domain mediating cell death in *Leishmania major*. *Mol. Microbiol.* **2011**, *79*, 222−239.
(30) Chowdhury, S.; Mukherjee, T.; Chowdhury, S. R.; Sengupta, S.; Mukhopadhyay, S.; Jaisankar, P.; Majumder, H. K. Disuccinyl betulin triggers metacaspase-dependent endonuclease g-mediated cell death in unicellular protozoan parasite *Leishmania donovani*. *Antimicrob. Agents Chemother.* **2014**, *58*, 2186−2201.
(31) Lee, N.; Gannavaram, S.; Selvapandiyan, A.; Debrabant, A. Characterization of Metacaspases with Trypsin-Like Activity and Their Putative Role in Programmed Cell Death in the Protozoan ParasiteLeishmania. *Eukaryotic Cell* **2007**, *6*, 1745−1757.
(32) Dolai, S.; Pal, S.; Yadav, R. K.; Adak, S. Endoplasmic reticulum stress-induced apoptosis in leishmania through Ca^{2+}-dependent and caspase-independent mechanism. *J. Biol. Chem.* **2011**, *286*, 13638−13646.
(33) Reimão, J. Q.; Miguel, D. C.; Taniwaki, N. N.; Trinconi, C. T.; Yokoyama-Yasunaka, J. K. U.; Uliana, S. R. B. Antileishmanial activity of the estrogen receptor modulator raloxifene. *PLoS Neglected Trop. Dis.* **2014**, *8*, e2842.
(34) Fonseca-Silva, F.; Inacio, J. D. F.; Canto-Cavalheiro, M. M.; Almeida-Amaral, E. E. Reactive oxygen species production and mitochondrial dysfunction contribute to quercetin induced death in *Leishmania amazonensis*. *PLoS One* **2011**, *6*, e14666.
(35) Banki, K.; Hutter, E.; Gonchoroff, N. J.; Perl, A. Elevation of mitochondrial transmembrane potential and reactive oxygen intermediate levels are early events and occur independently from activation of caspases in Fas signaling. *J. Immunol* **1999**, *162*, 1466−1479.
(36) Akaike, T.; Maeda, H. Nitric oxide and virus infection. *Immunology* **2000**, *101*, 300−308.
(37) Nathan, C.; Shiloh, M. U. Reactive oxygen and nitrogen intermediates in the relationship between mammalian hosts and microbial pathogens. *Proc. Natl. Acad. Sci. U.S.A.* **2000**, *97*, 8841−8848.
(38) Brunet, L. R. Nitric oxide in parasitic infections. *Int. Immunopharmacol.* **2001**, *1*, 1457−1467.
(39) Clark, I. A.; Rockett, K. A. Nitric oxide and parasitic disease. *Adv. Parasitol.* **1996**, *37*, 1−56.
(40) Wyllie, S.; Patterson, S.; Fairlamb, A. H. Assessing the essentiality of *Leishmania donovani* nitroreductase and its role in nitro drug activation. *Antimicrob. Agents Chemother.* **2013**, *57*, 901−906.
(41) Kucuksayan, E.; Ozben, T. Hybrid compounds as multitarget directed anticancer agents. *Curr. Top. Med. Chem.* **2017**, *17*, 907−918.
(42) Zhan, P.; Pannecouque, C.; De Clercq, E.; Liu, X. Anti-hiv drug discovery and development: Current innovations and future trends. *J. Med. Chem.* **2016**, *59*, 2849−2878.
(43) Otero, E.; García, E.; Palacios, G.; Yepes, L. M.; Carda, M.; Agut, R.; Vélez, I. D.; Cardona, W. I.; Robledo, S. M. Triclosan-caffeic acid hybrids: Synthesis, leishmanicidal, trypanocidal and cytotoxic activities. *Eur. J. Med. Chem.* **2017**, *141*, 73−83.
(44) Baquedano, Y.; Moreno, E.; Espuelas, S.; Nguewa, P.; Font, M.; Gutierrez, K. J.; Jiménez-Ruiz, A.; Palop, J. A.; Sanmartín, C. Novel hybrid selenosulfonamides as potent antileishmanial agents. *Eur. J. Med. Chem.* **2014**, *74*, 116−123.
(45) Somaratne, V. N.; Ranawaka, R. R.; Jayaruwan, H. M.; Wipuladasa, D. M.; de Silva, S. H. P. Randomized, double-blind study on intralesional metronidazole versus intralesional sodium stibogluconate in *Leishmania donovani* cutaneous leishmaniasis. *J. Dermatol. Treat.* **2019**, *30*, 87−91.
(46) Gangneux, J.-P.; Dullin, M.; Sulahian, A.; Garin, Y. J.-F.; Derouin, F. Experimental evaluation of second-line oral treatments of visceral leishmaniasis caused by *Leishmania infantum*. *Antimicrob. Agents Chemother.* **1999**, *43*, 172−174.
(47) del Estal, P. L.; Moya, M. S.; Martin, T.; Lucero, M. J.; Salgado, R. Metronidazole therapy for visceral leishmaniasis. *Clin. Infect. Dis.* **1994**, *19*, 1161−1162.
(48) Bianciardi, P.; Fasanella, A.; Foglia Manzillo, V.; Trotta, T.; Pagano, A.; Sorino, S.; Gradoni, L.; Oliva, G. The efficacy of enrofloxacin, alone or combined with metronidazole, in the therapy of canine leishmaniasis. *Parasitol. Res.* **2004**, *93*, 486−492.
(49) Löfmark, S.; Edlund, C.; Nord, C. E. Metronidazole is still the drug of choice for treatment of anaerobic infections. *Clin. Infect. Dis.* **2010**, *50*, S16−S23.
(50) Nakayama, H.; Loiseau, P. M.; Bories, C.; Torres de Ortiz, S.; Schinini, A.; Serna, E.; Rojas de Arias, A.; Fakhfakh, M. A.; Franck, X.; Figadere, B.; Hocquemiller, R.; Fournet, A. Efficacy of orally administered 2-substituted quinolines in experimental murine cutaneous and visceral leishmaniases. *Antimicrob. Agents Chemother.* **2005**, *49*, 4950−4956.
(51) Yousuf, M.; Mukherjee, D.; Dey, S.; Pal, C.; Adhikari, S. Antileishmanial ferrocenylquinoline derivatives: Synthesis and biological evaluation against *Leishmania donovani*. *Eur. J. Med. Chem.* **2016**, *124*, 468−479.
(52) Ukil, A.; Biswas, A.; Das, T.; Das, P. K. 18 -Glycyrrhetinic Acid Triggers Curative Th1 Response and Nitric Oxide Up-Regulation in

DOI: 10.1021/acs.jmedchem.9b00628
J. Med. Chem. XXXX, XXX, XXX−XXX

Experimental Visceral Leishmaniasis Associated with the Activation of NF- B. *J. Immunol.* **2005**, *175*, 1161−1169.
(53) Sharma, G.; Kar, S.; Basu Ball, W.; Ghosh, K.; Das, P. K. The curative effect of fucoidan on visceral leishmaniasis is mediated by activation of map kinases through specific protein kinase c isoforms. *Cell. Mol. Immunol.* **2014**, *11*, 263−274.
(54) Kyriazis, I. D.; Koutsoni, O. S.; Aligiannis, N.; Karampetsou, K.; Skaltsounis, A.-L.; Dotsika, E. The leishmanicidal activity of oleuropein is selectively regulated through inflammation- and oxidative stress-related genes. *Parasites Vectors* **2016**, *9*, 441.
(55) Verma, N. K.; Singh, G.; Dey, C. S. Miltefosine induces apoptosis in arsenite-resistant *Leishmania donovani* promastigotes through mitochondrial dysfunction. *Exp. Parasitol.* **2007**, *116*, 1−13.
(56) Shadab, M.; Jha, B.; Asad, M.; Deepthi, M.; Kamran, M.; Ali, N. Apoptosis-like cell death in *Leishmania donovani* treated with kalsometm10, a new liposomal amphotericin b. *PLoS One* **2017**, *12*, e0171306.
(57) Félix, M. B.; de Souza, E. R.; de Lima, M. d. C. A.; Frade, D. K. G.; Serafim, V. d. L.; Rodrigues, K. A. d. F.; Néris, P. L. d. N.; Ribeiro, F. F.; Scotti, L.; Scotti, M. T.; de Aquino, T. M.; de Oliveira, M. R.; de Oliveira, M. R. Antileishmanial activity of new thiophene-indole hybrids: Design, synthesis, biological and cytotoxic evaluation, and chemometric studies. *Bioorg. Med. Chem.* **2016**, *24*, 3972−3977.
(58) Ramu, D.; Garg, S.; Ayana, R.; Keerthana, A. K.; Sharma, V.; Saini, C. P.; Sen, S.; Pati, S.; Singh, S. Novel *β*-carboline-quinazolinone hybrids disrupt Leishmania donovani redox homeostasis and show promising antileishmanial activity. *Biochem. Pharmacol.* **2017**, *129*, 26−42.
(59) Baréa, P.; Barbosa, V. A.; Bidóia, D. L.; de Paula, J. C.; Stefanello, T. F.; da Costa, W. F.; Nakamura, C. V.; Sarragiotto, M. H. Synthesis, antileishmanial activity and mechanism of action studies of novel *β*-carboline-1,3,5-triazine hybrids. *Eur. J. Med. Chem.* **2018**, *150*, 579−590.
(60) Ashutosh; Gupta, S.; Ramesh; Sundar, S.; Goyal, N. Use of *Leishmania donovani* field isolates expressing the luciferase reporter gene in in vitro drug screening. *Antimicrob. Agents Chemother.* **2005**, *49*, 3776−3783.
(61) Anand, D.; Yadav, P. K.; Patel, O. P. S.; Parmar, N.; Maurya, R. K.; Vishwakarma, P.; Raju, K. S. R.; Taneja, I.; Wahajuddin, M.; Kar, S.; Yadav, P. P. Antileishmanial activity of pyrazolopyridine derivatives and their potential as an adjunct therapy with miltefosine. *J. Med. Chem.* **2017**, *60*, 1041−1059.
(62) Das, R.; Roy, A.; Dutta, N.; Majumder, H. K. Reactive oxygen species and imbalance of calcium homeostasis contributes to curcumin induced programmed cell death in *Leishmania donovani*. *Apoptosis* **2008**, *13*, 867−882.
(63) Vishwakarma, P.; Parmar, N.; Yadav, P. K.; Chandrakar, P.; Kar, S. 15d-prostaglandin j2 induced reactive oxygen species-mediated apoptosis during experimental visceral leishmaniasis. *J. Mol. Med.* **2016**, *94*, 695−710.
(64) Huber, W.; Koella, J. C. A comparison of three methods of estimating ec50 in studies of drug resistance of malaria parasites. *Acta Trop.* **1993**, *55*, 257−261.
(65) Kulkarni, M. M.; McMaster, W. R.; Kamysz, W.; McGwire, B. S. Antimicrobial Peptide-induced Apoptotic Death ofLeishmaniaR-esults from Calcium-de pend ent, Caspase-independent Mitochon-drial Toxicity. *J. Biol. Chem.* **2009**, *284*, 15496−15504.
(66) Vishwakarma, P.; Parmar, N.; Chandrakar, P.; Sharma, T.; Kathuria, M.; Agnihotri, P. K.; Siddiqi, M. I.; Mitra, K.; Kar, S. Ammonium trichloro [1,2-ethanediolato-O,O′]-tellurate cures experimental visceral leishmaniasis by redox modulation of Leishmania donovani trypanothione reductase and inhibiting host integrin linked PI3K/Akt pathway. *Cell. Mol. Life Sci.* **2018**, *75*, 563−588.
(67) Kathuria, M.; Bhattacharjee, A.; Sashidhara, K. V.; Singh, S. P.; Mitra, K. Induction of mitochondrial dysfunction and oxidative stress in *Leishmania donovani* by orally active clerodane diterpene. *Antimicrob. Agents Chemother.* **2014**, *58*, 5916−5928.
(68) XXIV, U. P. *The United State of Pharmacopoeia Convention*, Rockville, Maryland, 2000; p 185.
(69) Chhonker, Y. S.; Sleightholm, R. L.; Murry, D. J. Bioanalytical method development and validation of moxidectin in plasma by LC-MS/MS: Application to in vitro metabolism. *Biomed. Chromatogr.* **2019**, *33*, e4389.
(70) Liu, H.; Huang, Z.; Li, H.; Zhang, Q.; Tan, X.; Lu, F.; Li, S. Characterization of preclinical in vitro and in vivo pharmacokinetics properties for kbp-7018, a new tyrosine kinase inhibitor candidate for treatment of idiopathic pulmonary fibrosis. *Drug Des., Dev. Ther.* **2015**, *9*, 4319−4328.

DOI: 10.1021/acs.jmedchem.9b00628
J. Med. Chem. XXXX, XXX, XXX−XXX